AD-A057 564 TRINITY COLL DUBLIN (IRELAND) SCHOOL OF ENGINEERING F/G 11/2
FLEXURAL STRENGTH OF REINFORCED MICROCONCRETE IN STATIC AND IMP--ETC(U)
MAR 78 T E GLYNN, M Z AL-SALIHI, R J MEAGHER DA-ERO-75-G-030

UNCLASSIFIED NL

1 OF 1
ADA
057564

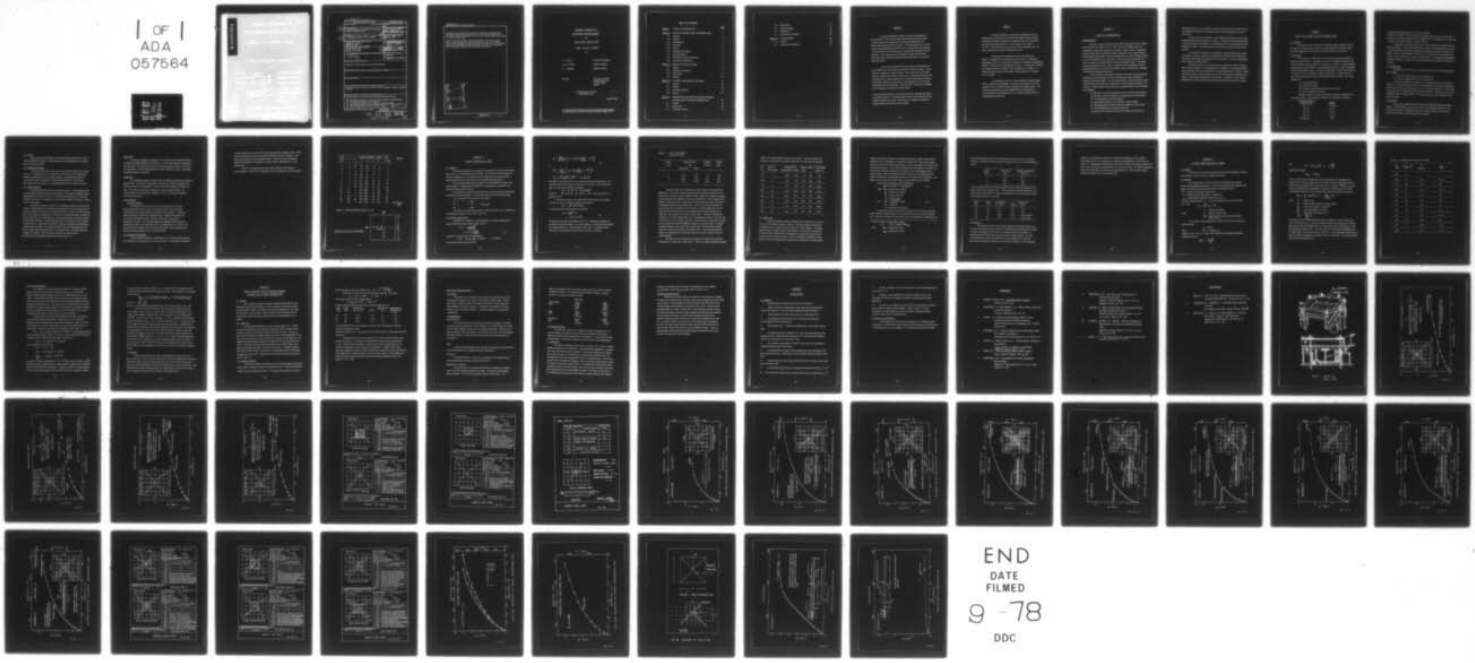

END
DATE
FILMED
9-78
DDC

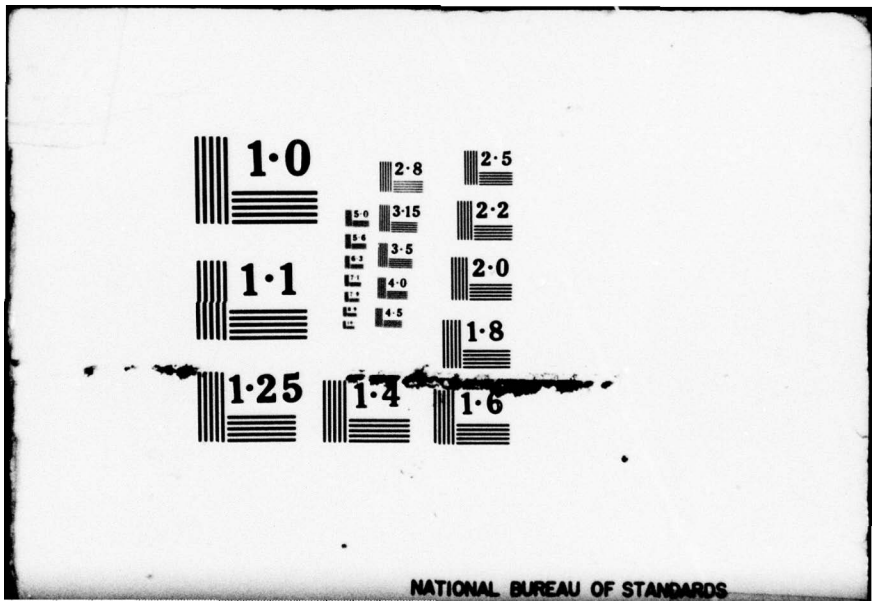
1·0
1·1
1·25
1·4
1·6
1·8
2·0
2·2
2·5
2·8
3·15
3·5
4·0
4·5
NATIONAL BUREAU OF STANDARDS

UNCLASSIFIED

SECURITY CLASSIFICATION OF THIS PAGE (When Data Entered)

REPORT DOCUMENTATION PAGE	READ INSTRUCTIONS BEFORE COMPLETING FORM
1. REPORT NUMBER	2. GOVT ACCESSION NO. 3. RECIPIENT'S CATALOG NUMBER
4. TITLE (and Subtitle) FLEXURAL STRENGTH OF REINFORCED MICROCONCRETE IN STATIC AND IMPACT TESTS.	5. TYPE OF REPORT & PERIOD COVERED FINAL TECHNICAL REPORT. JUNE 75 — MARCH 78, 6. PERFORMING ORG. REPORT NUMBER
7. AUTHOR(s) T.E. GLYNN, M.Z. AL-SALIHI, R.J. MEAGHER	8. CONTRACT OR GRANT NUMBER(s) DAERO-75-G-030 new
9. PERFORMING ORGANIZATION NAME AND ADDRESS UNIVERSITY OF DUBLIN ENGINEERING SCHOOL TRINITY COLLEGE, DUBLIN, IRELAND	10. PROGRAM ELEMENT, PROJECT, TASK AREA & WORK UNIT NUMBERS 6.11.02A;1M161102B52B;00-382
11. CONTROLLING OFFICE NAME AND ADDRESS US ARMY R&S GP (EUR) BOX 65, FPO NY 09510	12. REPORT DATE MARCH 1978 13. NUMBER OF PAGES 54
14. MONITORING AGENCY NAME & ADDRESS (if different from Controlling Office) 63p.	15. SECURITY CLASS. (of this report) UNCLASSIFIED 15a. DECLASSIFICATION/DOWNGRADING SCHEDULE

16. DISTRIBUTION STATEMENT (of this Report)

Approved for Public Release; Distribution Unlimited.

17. DISTRIBUTION STATEMENT (of the abstract entered in Block 20, if different from Report)

18. SUPPLEMENTARY NOTES

19. KEY WORDS (Continue on reverse side if necessary and identify by block number)

Reinforced concrete; Stress on concrete; tensile strengths; flexural strengths of beams.

20. ABSTRACT (Continue on reverse side if necessary and identify by block number)

The final report on this investigation addresses these objectives:

(a) The static resistance of slabs with varying amounts of reinforcement,
(b) The development of yield line patterns,
(c) The dynamic resistance of the slabs due to impact loading,
(d) Relationship between static and dynamic deformation of thin slabs, and
(e) Slab strengthening by composite construction.

PTO

DD FORM 1 JAN 73 1473 EDITION OF 1 NOV 65 IS OBSOLETE

UNCLASSIFIED

SECURITY CLASSIFICATION OF THIS PAGE (When Data Entered)

One reason for the inclusion of the dynamic resistance is the fact that reinforced concrete(in various forms) is now used in the construction of ships hulls and the classification societies are including some form of impact as a quality control test.

A total of 12 static loading tests were performed on 40 and 25 mm thick slabs. Impact loading tests were performed on 12 slabs. A theoretical study of concrete slabs of arbitrary curvature was undertaken. The stiffness matrix for curved elements will be presented in a thesis. The theoretical study is devoted to concrete shells of arbitrary curvature.

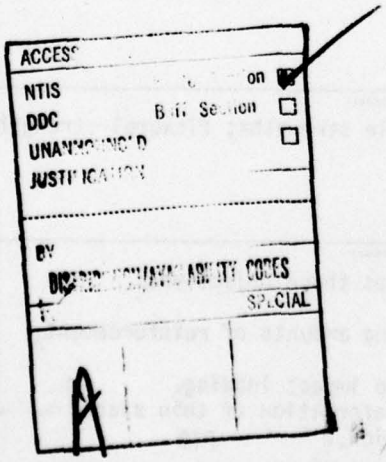

FLEXURAL STRENGTH OF REINFORCED MICROCONCRETE IN STATIC AND IMPACT TESTS

FINAL TECHNICAL REPORT

by

T. E. Glynn	Principal Investigator
M. Z. Al-Salihi	Research Assistant
R. J. Meagher	Research Assistant

Grantee

University of Dublin
Engineering School
Trinity College
Dublin

European Research Office,
United States Army.

MARCH 1978.

The research reported in this document has been made possible through the support and sponsorship of the United States Army through its European Research Office.

TABLE OF CONTENTS

		Page
Chapter I	SCOPE OF INVESTIGATION	1
Chapter II	STATIC AND IMPACT TESTS ON SQUARE SLABS	3
2.1	General	3
2.2	Concrete	3
2.3	Reinforcement	4
2.4	Formwork	4
2.5	Curing	5
2.6	Preparation for Testing	5
2.7	Testing Procedure	6
2.8	Test Results - Yield Line Patterns	7
2.9	Discussion of Test Results	7
Chapter III	ELASTIC ANALYSIS OF SLABS	8
3.1	General	8
3.2	Analysis of Test Results	8
3.3	Impact Tests	11
3.4	Summary	13
Chapter IV	ULTIMATE LOAD ANALYSIS OF SLABS	15
4.1	General	15
4.2	Analysis	15
4.3	Discussion of Results	17
4.4	Summary	18
Chapter V	SPECIAL AND PILOT TESTS ON SLABS AND BEAMS. DYNAMIC TEST ON AGED CONCRETE SLAB	19
5.1	General	19
5.2	Impact Tests	19
5.3	Discussion of Results	19

5.4	Specification	21
5.5	Testing Procedure	21
5.6	Test Results	22
5.7	Discussion of Test Results	23
Chapter VI	CONCLUSIONS	24
6.1	General	24
6.2	Areas for Future Research	25

ABSTRACT

This report presents the results of a laboratory investigation of the behaviour of thin concrete slabs under static and impulsive loading. The main variable was the quantity of wire mesh reinforcement in the tensile zone produced by flexural testing. The slabs measured 750 x 750 mm in plan and had thicknesses of 25 and 40 mm. Reinforcement varied between 0.4 and 1.8 per cent of the gross area of concrete and unreinforced control specimens. Static loading was accomplished by hydraulic jacking tests, and the impulsive load tests employed falling weight impact. A total of 25 slabs were tested.

The test results indicated that the quantity of reinforcement has only a slight effect on the load that is required to initiate cracking. On the load that is required to initiate cracking. On the other hand, the ultimate strength is strongly influenced by the steel ratio. Analysis of the test data has demonstrated that a good correlation exists between experimental results and conventional reinforced concrete theory; where disparity occurs the theory underestimates the actual strength. The impact tests results serve to highlight the low resistance of concrete to impulsive loads.

To improve impact resistance, tests were performed on composite steel plate-concrete slab sections. A very significant increase in static resistance of the composite members was noted. Further work is in progress on a program of testing composite sections with impact loading.

PREFACE

The research described in this report was performed in Trinity College Dublin under Grant No. DA-ERO-75-G-030 for project entitled "Investigation of Stress Concentration in Reinforced Concrete Components". The work was conducted for the U.S. Army under R. & D. Project No. 2171. The report covers the period June 1975 to December 1977, and forms a continuation of earlier work reported in 1975.

A large part of the experimental work was performed by Richard J. Meagher while on sabbatical leave from the S.A. Institute of Technology, Australia. The principal investigator was assisted by postgraduate student P. Donelan and by undergraduates D. Lewis, P. Power and D. Hartford. The analysis presented in Chapter IV was undertaken by P. Donelan. A theoretical study of arbitrary shell shapes is being presented in a thesis by M. Z. Al Salihi.

The sponsorship of the U.S. Army through the European Research Office is gratefully acknowledged. The authors are indebited to Dr. Hoyt Lemons of E.R.O. staff for his advice throughout the research project. The technical assistance and materials supplied by Cement Roadstone Ltd., Loctite (Ireland), Shell Composites Ltd., and Tinsley Wire (Ireland) Ltd. is acknowledged with gratitude.

CHAPTER I

SCOPE OF INVESTIGATION

INTRODUCTION

This report covers the period from June 1975 to December 1977 for research under Grant No. DA - ERO - 75 - G - 030. The research reported herein is a continuation of the project described in two previous reports entitled "Investigation of Stress Concentration in Reinforced Concrete Components" and "Tensile Strength of Reinforced Microconcrete", which were submitted to the European Research Office in July 1974 and August 1975 respectively. The previous reports have dealt with stress concentrations, tensile strengths and flexural strengths of beams. The tensile tests were performed on one way slabs. The beam tests were performed on simply supported specimens which utilised three different types of reinforcement, weldmesh, chickenmesh and expanded metal sheet.

At the conslusion of the research relating to beam tests it was observed that weldmesh was the most satisfactory type for providing the tensile component of resistance in flexural members. It was resolved that further research should be undertaken utilising welded steel mesh reinforcement in flexural members spanning in two directions. Simply supported square slabs were considered adequate for the proposed test programme.

The objectives of the testing programme were to determine the following:

(a) The static resistance of slabs with varying amounts of reinforcement.

(b) The development of yield line patterns.

(c) The dynamic resistance of the slabs due to impact loading.

(d) Relationship between static and dynamic deformation of thin slabs.

(e) Slab strengthening by composite construction.

One reason for the inclusion of the dynamic resistance is the fact that

reinforced concrete (in various forms) is now used in the construction of ships hulls and the classification societies are including some form of impact resistance as a quality control test.

A total of 12 static loading tests were performed on 40 and 25 mm thick slabs. Impact loading tests were performed on 12 slabs. A theoretical study of concrete slabs of arbitrary curvature was undertaken. The stiffness matrix for curved elements will be presented in a thesis. The theoretical study is devoted to concrete shells of arbitrary curvature.

It was desired to undertake an investigation of self-stressing by use of expansive cements. Whilst the materials are commercially available in the United States, no source of local supply could be found for bulk quantities. The study was abandoned after completion of a few pilot tests.

Some of the earlier work concentrated on the influence of helical reinforcement on flexural strength. The investigation proved negative as no measurable effects were derived from helical reinforcement for flexure or direct tension. However, helical reinforcement serves a useful purpose in that it serves as both shear reinforcement and a spacer for controlling the thickness of 'lay-up' slabs. In Chapter V a new process is described where helical binding could facilitate placement of concrete in thin shells.

CHAPTER II

STATIC AND IMPACT TESTS ON SQUARE SLABS

2.1 General

The static tests were carried out by applying a single concentrated load at the centre of a square micronconcrete slab, simply supported along all four edges. The central deflection and the strains in the tensile surface were measured.

2.2. Concrete

The concrete mix utilised was that which has been previously reported as achieving maximum density. Aggregates were sound, well graded sedimentary rock which were dried, sieved and stored in a dry state until required. A rapid hardening Portland cement of Irish manufacture was employed for all tests. Water was obtained direct from the domestic supply. Materials were batched by weight, and in addition, the volume of water was measured. Mixing was performed in a paddle type drum mixer which was washed out and drained immediately prior to mixing. The mixing sequence was :

(i) mix for five minutes

(ii) remove mixing head

(iii) scrape any accumulated fines from the drum walls

(iv) mix for a further two minutes

Sufficient material was mixed in each batch to produce concrete for one slab and test cubes. An aliquot batch consisted of mix proportions as follows :

Aggregate Retained on BS SIEVE NO	WEIGHT
No. 7	16.30 kg
No. 14	12.20 "
No. 25	6.10 "
No. 52	4.10 "
Passing 52	2.00 "

12.8 kg of rapid hardening cement and 5.76 kg of water
yield of mix 0.0283 m^3. The test cubes were vibrated, the mass of each cube being in excess of 8 kg and the density in excess of 2380 kg m^{-3}. The strengths of the cubes were in excess of 50 N/mm^2 at 28 days (cube size 150 mm).

Compaction of the concrete with layers of closely spaced mesh presented several practical problems. In the case of the 25 mm mesh with 5 mm spacing between the layers, it was found that the mesh could be plastered and subsequently vibrated to achieve compaction. When the same mesh was utilised with a 2.5 mm spacing it was extremely difficult to work the material into the mesh, and furthermore, it was observed that segregation occurred on vibration. Similar, but less acute problems were encountered utilising the 12 mm mesh.

2.3 Reinforcement

Reinforcement was of two sizes of welded steel mesh which had been galvanised after welding.

i) 25 mm (1") square grid of 1.66 mm diameter wire

ii) 13 mm ($\frac{1}{2}$") square grid of 0.97 mm diameter wire

The mesh was supplied in rolled form, it was trimmed to size and carefully hand flattened. A predetermined number of layers were assembled, spacing being achieved by means of either 5 mm thick perspex blocks, or 2.5 mm vinyl tile segments. The reinforcement and spacers were adequately held in place with wire ties. Bottom cover of 5 mm was provided by means of perspex blocks. The mat was placed with the wires parallel to the edges of the slab.

2.4 Formwork

The formwork consisted of a base of multi-ply chipboard and mild steel angle sections. A smooth finish on one face of the slab was achieved by covering the chipboard with heavy plastic sheeting and casting the concrete directly onto the plastic. The mould was placed on a vibrating table during casting.

2.5 Curing

Slabs and cubes were stripped 24 hours after placing, and cured in a water tank until required for testing. Curing took place at room temperature as no temperature control was provided.

2.6 Preparation for testing

The slabs were removed from the water tank and surface dried with a current of hot air. The tensile face was scrubbed with a wire bruch to yield a high quality finish (thus enabling cracks to be readily detected). A square grid was drawn on one side of the slab for the purpose of referencing yield lines to a 100 mm grid. Strain gauges were cemented in two orthogonal directions at the centre of the slab.

2.7 Testing Procedure

A purpose designed rig was built for the flexure tests. In some pilot tests the load was applied vertically from above the specimen. This procedure suffered from the disadvantage that the tension face, with the reference grid marked on it, was on the underside of the slab, and consequently was not readily available for scrutiny. This procedure was abandoned.

The majority of slabs were tested in a rig modified to apply the load vertically upwards. A levelling base was provided by placing the slab on four bolt heads and the bolts were adjusted until all four were tight and slab level. A layer of mortar (sand and high alumina cement) was applied over a width of 75 mm around the edges, and channel sections and taken down to base members. The rods were tightened to hold the channel sections firmly in position. The clear dimension of the slab inside the channel sections was 600 x 600 mm. Loading was by means of a hydraulic prestressing jack operated by a single acting hand pump. The load was measured using a pressure gauge which had been previously calibrated with the jack in a testing machine. The loading head was a segment of a sphere of 150 mm diameter machined to a radius of 25 mm. The layout of the testing rig for static tests is shown in FIG. II.1.

Static Tests

The load was applied in increments of 1 kilo-newton and the central deflection recorded when stable deflection was attained i.e. initial creep included in measurement. The tension face was examined for cracks which were progressively marked on the slab as they developed. A strong magnifying glass was used to locate the cracks. Strain gauge readings were taken in some tests.

Impact Tests

The loading head used for the static tests was modified by adding lead weights for impact testing. The impactor was permitted a free drop by cutting the suspension wire. The drop was preset by a gauge block. For the 40 mm slabs a weight of 47.80 kg. was used. The 25 mm thick slabs were subjected to a droping weight of 33 kg. The contact surface of the impactor had a diameter of 12 mm. The impact was applied at the centre of the slab.

2.8 Test Results

Yield Line Patterns

The object of the static tests was that the slabs should fail in flexure. This was achieved in all but one case, that being the test on the most heavily reinforced slab which also produced an extensive yield line pattern. Yield lines mostly produced the characteristic diagonal pattern. Single lines radiated from the centre and generally branched into three within 50 mm of the point of application of the load. The yield line patterns are displayed with the details of the loading in FIGS. II-2 through FIG. II-20. The diagrams FIG. II-2 to FIG. II-8 pertain to static and impact tests on the 25 mm thick slabs. The test results for the 40 mm thick slabs are shown in FIG. II-9 to FIG.II-20.

2.9 Discussion of Test Results

The test specimens provided a consistent set of results which enable evaluation of the behaviour of microconcrete in two-way slab action. The behaviour is evaluated

in terms of deflection, stress at initial cracking and ultimate collapse moments. Strain gauge measurements for the most part proved unreliable as shown in Table 2.1; the strain measurements are not fully reported herein. However the strain readings do indicate that deflection is localized to a circular area of radius 200 mm, i.e. the effective span.

The area of reinforcement had only a slight influence on the loads for initial cracking. The effect of a reinforcement is most noticeable in ultimate strength.

LOAD (kN)	STRAIN GAUGES ($\mu\epsilon$) 1	2	3	4	5	6	DEFL. 10^{-2}mm	Remarks
1	0	35	20	30	0	0	1	
2	0	-5	10	40	0	0	2	
3	0	0	70	75	10	0	4	
4	0	25	80	95	10	0	6	
5	0	10	120	125	15	0	8	
6	0	10	155	150	25	0	10	
9	5	20	200	340	25	-10	18	
12	5	20	180	1130	20	-20	31.5	
15	-15	5	190	2000	15	-40	48	
18	-35	-5	280	3200	20	-70	72	
21	-50	0	300	4400	65	-80	102	
24	-80	-30	480	6000	85	-110	156	
27	-105	-5	600	8100	95	-130	231	yield lines to edges

TABLE 2.1 STRAIN READINGS SLAB NO. 102

LOCATIONS OF GAUGES

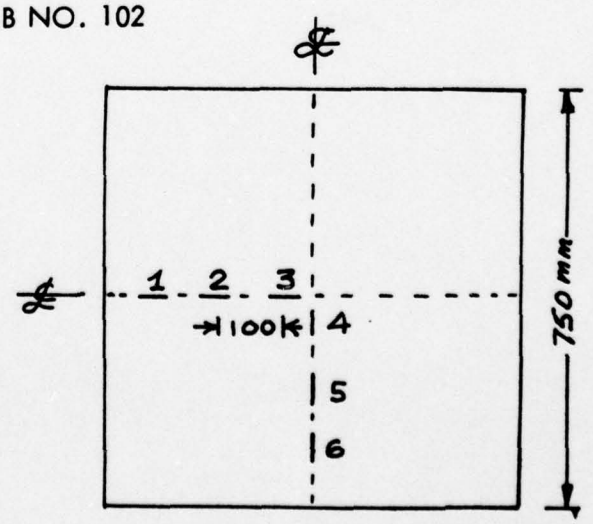

CHAPTER III

ELASTIC ANALYSIS OF SLABS

3.1 General

The analyses presented in this chapter will concentrate on the static and impact tests carried out on the slabs of 25 mm thickness. Test results for the 40 mm slabs will serve as a comparison with the limitation that the thicker slab is more susceptible to shear deformation which complicates an analysis based flexural behaviour.

The theoretical deflections are compared with the experimental values in the elastic regime, i.e. deflections that correspond to loads less than, or equal to, the load that initiates visible cracking.

The slabs (25 mm thick) were reinforced with two sizes of galvanised weld mesh denoted by 13 and 25 mm square. The eight slabs tested were reinforced as follows:

(a) Two number with two layers of 13 mm mesh.

(b) " " " three " " " "

(c) " " " two " " 25 mm mesh.

(d) " " " three " " " "

The results of the static tests are shown in FIG II-2 to FIG. II-5. The results of the impact tests are given in FIG. II-6 to FIG. II-8.

3.2 Analysis of Static Tests

The deflection caused by a concentrated load on a simply supported slab is given by Roark and Young (1975) pp 386 in the form:

$$w = \frac{-\alpha P b^2}{E t^3}$$

$$= 0.12 \frac{P b^2}{E t^3} \qquad (1)$$

Therefore for the slab size of this investigation

$$w = 2.76 \frac{P}{E} \quad [mm] \quad ; \quad P[kN]$$

The maximum bending stress is given by

$$\sigma = \frac{3P}{2\pi t^2}\left[(1+\nu)\ln\frac{2b}{\pi r_o'} + \beta\right] \qquad (2)$$

or

$$\sigma = \frac{1.5}{\pi t^2}\left[1.2\ln\frac{2b}{\pi r_o'} + \beta\right]P$$

$$r_o' = \sqrt{1.6r_o^2 + t^2} - 0.675t$$

where r_o' is the actual radius of the contact surface of the loading head. The equivalent radius r_o' depends on the thickness t of the slab. Thus for the 25 mm slabs the stress given by equation 2 reduces to

$$\sigma = 3.37\,P \quad [N/mm^2]$$

for $\nu = 0.2$, $r_o' = 9.25$ mm, $b = 400$ mm, $\beta = 0.435$ and the load P is specified in kN.

Our earlier research on the stress-strain relationship of microconcrete indicates the value of the elastic modulus is of the order

$$E = 30\ kN/mm^2$$

The maximum strain is obtained from the expression

$$\epsilon = \frac{1-\nu}{E}\sigma = 27\times10^{-6}\sigma \qquad (3)$$

The static test results are summarised in FIG. III-1. This diagram indicates that the specimens behaved similarly up to initial cracking. For the analytical purposes the average deflection vs. load is plotted in FIG. III-2. A comparison of the theoretical and experimental results is shown in Table 3.1 overpage.

TABLE 3.1 STATIC TEST RESULTS
(25 mm thick slabs)

LOAD (kN)	DEFLECTIONS (mm)		STRESS N/Mm^2	STRAIN $\mu\varepsilon$
	Experiment	Theory		
2	0.12	0.18	6.7	180
4	0.30	0.37	13.5	360
6	0.60	0.55	20.2	540

These data indicate good agreement between theoretical and experimental deflections. On the other hand the computed stress and strains are higher than the actual stress that would initiate cracking in a beam. Reference to equation 2 suggests that the presence of the singularity within the bracketed term, which exaggerates the stresses for small r_o' values, could account for high theoretical values of the stress in the neighbourhood of the concentrated load. The two-way concrete slab does not exactly qualify for the definition of a thin plate. It is quite possible that the same deflection would be measured if the concentrated load had been distributed on a larger area, for instance, over an area of radius 50 mm. The stress would then be computed as 12 N/mm^2 approximately with a corresponding reduction in the strain due to less curvature in the vicinity of the load. The study seems to confirm that the allowable working stress of 7N/mm^2 (1000 psi) proposed in our earlier report, is justified for design purposes, Glynn and Al Salihi (1975) pp 34. No detrimental cracking under static load would develop for this design value. When load cracks become visible it is considered that working stress theory has no further bearing on the calculated response.

The slabs of 40 mm thickness were analysed on the basis that the load was distributed over a square area of side 100 mm. Again the theoretical deflections agreed

closely with the experimental values as shown below. It may be noted from the table that the values of the computed stresses are of the right order of magnitude.

SLAB No.	LOAD AT FIRST CRACK	DEFLECTIONS		STRESS N/mm^2	STRAIN	REINFORCE-MENT - %
		Experimental	Theory			
100	11	0.30	0.29	9.2	248	NIL
102	17	0.62	0.44	14.2	383	0.9%
103	13	0.31	0.33	10.9	294	0.9%
104	19	0.59	0.50	16.0	432	1.8%
105	14	0.41	0.35	11.8	318	0.9%
106	13	0.34	0.34	10.9	294	0.9%
107	13	0.34	0.34	10.9	294	0.9%
108	13	0.34	0.34	10.9	294	0.9%

3.3 Impact Tests

In the simple analysis of impact loading given in standard texts, the inertial mass of the structural member is ignored. The kinetic energy of the impactor is assumed to be all converted to strain energy of the elastic member. This simple analysis leads to an upper bound on the deflection. In this section the behaviour of concrete slabs in flexure will be investigated for loads which are less than the dynamic load that initiates cracking. Firstly we will apply the elementary theory and later review its implications for analysis with the refinement of inertial effects.

Indeed there have been attempts to use elementary theory to analyse concrete beams subjected to plastic deformation, Cracknell and Jarman (19). These authors adopted expressions from Simms (1943) which indluded the ratio of the weight of the beam to the weight of the impactor.* Use of Simms reduction factor was deemed to account for the loss of kinetic energy in crushing of the concrete, strain in the steel, rebound and acoustic energy. Even in application of elastic theory it is a prerequisite that the weight of the striker is an appreciable fraction of the weight of the anvil member. The objective of this section is to relate dynamic impact loading to static loading.

The governing equations of impact loading are:

$$W_m (S + \delta) = \frac{1}{2} K \delta^2 \qquad (4)$$

where W_m = weight of the impactor

S = free drop of impactor

δ = dynamic deflection

K = spring constant

and $m = \sqrt{2gS}\, W_m \qquad (5)$

m = momentum

g = gravitional acceleration

To analyse the dynamic test data for the slabs of 25 mm thickness the spring constant defined as deflection per unit load was derived from the results of the static tests. Similar to the trend of the static test results, the dynamic tests yielded date that

---

* The Simm's Reduction factor takes the form:

$$\alpha = 1/(1 + 4/5)\, W_b/W_m$$

where W_b = weight of the beam

W_m = weight of the striker

are almost identical for each of the four slabs shown in Fig. II-6 to 8. The spring constant of the slabs in the flexural mode is derived from Fig. III-1 with the following results:

LOAD (kN)	DEFLECTION (mm)	SPRING CONSTANT (kN/mm)
2	0.12	16.7
4	0.30	13.3
6	0.60	10.0

It may be observed that no cracking was evident when the slabs were subjected to an impact mass of 33 kg dropping 75 mm. All the specimens exhibited detectable cracks when the drop reached 100 mm. Based on Equations (4) and (5) the theoretical values of the dynamic response are as follows:

MASS (kg)	DROP (mm)	MOMENTUM kg.m. Sec.	K (kN/mm)	DEFLECTION (mm)
33	25	23.1	16.7	1.02
33	50	32.7	13.3	1.58
33	75	40.0	10.0	2.34 uncracked
33	100	46.2	10.0	2.58 cracked

3.4 Summary

The deflections calculated for impact loading are considerably greater than for the static loads that induces cracking. The relatively poor performance of concrete in impact is highlighted by the results. The analysis shows that it is difficult to estimate the actual stress in slabs caused by static and impact loading. The value of the analysis rests in the limits defined for the ratio of deflection to effective span and in the momentum of loads which will initiate cracking. From the foregoing

analysis it is concluded that cracking will develop if the deflection exceed 1/300 of the effective span or if the momentum of a impact load exceeds 40 kg. m/s (25 mm thick slabs). The correspondence between static and dynamic loading is most readily stated as the static load vs-momentum (provided that the mass involved in impact is a substantial proportion of the mass of the slab). The reinforcement percentages (0.5 to 1%) have only a slight influence on behaviour up to the cracking load.

CHAPTER IV

ULTIMATE LOAD ANALYSIS OF SLABS

4.1 General

The static tests on the 25 mm and 40 mm thick slabs are analysed for ultimate load conditions, and the results are compared with theory.

4.2 Analysis

The collapse load for each of the slabs was calculated using yield-line theory (assuming diagonal yield lines). Each slab was assumed simply supported at the edges, and consisting of isotropically reinforced rigid-plastic material.

If E = external work done by the point load

D = internal strain energy stored by yielding slab

m_n = normal ultimate moment/unit width for the slab

Then from energy principles, E = D and it has been shown by Jones and Wood (19) that

$$D = \sum_{1}^{k} m_n l \theta_n$$

where

k = number of yield lines

l = length of the yield line

θ_n = angle between the plate segment's adjacent to the yield line.

If we impose a virtual displacement of unity at the centre of a simply supported slab then

$$E = W_u \times 1$$

where W_u = Collapse Load

Referring to FIG. IV-1 (a), a slab at yield condition the angle between adjacent segments is given by:

$$\theta_n = \frac{2\sqrt{2}}{2}$$

and

$$D = 2m_n\sqrt{2} \cdot L \cdot 2\frac{\sqrt{2}}{L}$$

equating E with D get

$$W_u = 8m_n$$

Thus for a given slab the collapse load can be calculated from a knowledge of the geometry, or for a given collapse load, the thickness and amount of reinforcement for the slab can be calculated from ultimate load theory. Values of W_u/m_n for a great variety of loading and slab configurations are given by Mansfield (1957). For each of the slabs the value of m_n was calculated from ultimate load theory by the formula:

$$m_n = f_c' b d^2 q \left(1 - \frac{k_2}{k_1 k_3} q\right)$$

where b = width of slab

d = effective depth, depth to centroid of steel

f_y = yield stress of steel (= 250 N/mm^2)

f_c' = 0.8x cube strength of concrete

p = percentage reinforcement x 10^{-2}

$q = \frac{f_y}{f_c'} p$

The ultimate moment of beams and slabs failing by yielding of the steel is fairly insensitive to the values of k_1 k_2, and k_3 the constants relating to the geometry of the stress block of the concrete at ultimate load. The values were chosen to give $k_2/k_1k_3 = 0.59$. The experimental value of W_u was taken as that load at which the yield line pattern had fully formed. The results are shown in Table 4.1. In this table (page 16a) the slabs of thickness 25 mm are denoted by the numbers 122,123, 125 and 128. The remaining entries apply to slabs of thickness 40 mm.

TABLE 4.1 Collapse Load Characteristics of Slabs

SLAB No.	Collapse Load kN	m_n kNmm/mm	$\frac{W_u}{m_n}$
100	17		
102	27	1.65	16.4
103	24	1.09	22
104	31	2.05	15.1
105	25	1.14	22
106	25	1.14	22
107	24	1.60	15
108	24	1.60	15
122	12	0.36	33.3
123	11k	0.46	26
125	11	0.89	12.4
128	11	0.95	11.6

4.3 Discussion of Results

From Table 4.1 it will be seen that the values of W_u/m_n obtained greatly exceed the simple yield line value of $W_u/m_n = 8$. The principal reason for this discrepancy appears to be due to an underestimating the ultimate moment. Glynn & Al Salihi (1975) found in flexural tests on identical concrete beams with similar amounts of reinforcement that the ultimate bending moment was underestimated by 50 per cent. This concurs with the findings of Nervi and others. Reasons for the higher ultimate moment of microconcrete are the restraint offered by the lateral component of the reinforcement, the two-dimensional fixity, and the elimination of bond failure through the fine spacing of the mesh.

Another reason for the improved performance of the slabs was kinking of the reinforcement across the yield lines. Referring to Fig. IV-2, when the orientation of the steel differs from the direction of bending, in order for a valid yield mechanism to form the reinforcement must be bent across the yield line. A simple theory to explain this phenomenon is proposed by Wood (1961). If

and are the ultimate moment per unit width in two orthogonal directions, and the yield-line makes an angle to one of them, then assuming the reinforcement is kinked across the yield-line at right angles it follows that

$$m_n = m_1 \cos\theta + m_2 \sin\theta$$

For an isotropically reinforced slab

$$m_1 = m_2 = m$$

$$m_n = m(\cos\theta + \sin\theta)$$

or

$$\frac{m_n}{m} = \cos\theta + \sin\theta$$

The value of m_n/m is maximised when $\theta = 45^\circ$ and its value is equal to $(\sqrt{2})$ This theory implies a 40% increase in ultimate moment on planes with an inclination of 45° to the direction of reinforcement. In practice, however, the reinforcement will not be bent at right angles across the yield-line, due to crushing of concrete

as the bars tend to straighten themselves out. Kiviecinski (1965) formulated a theory of partial kinking of reinforcement across the yeild-line. The formula due to Kiviecinski takes the form:

$$\frac{m_n}{m} = \sqrt{1 + A^2 \sin^2\theta + \cos\theta} + \sqrt{1 - A^2 \cos^2\theta \sin\theta}$$

where $A = \sqrt{2 - \mu^2}$

and μ is an experimentally determined factor which is equal to $\frac{m_n}{m}$ for $\theta = 45^\circ$.

It can be shown that both Woods' complete kinking theory and the conventional "square" yield criterion are limiting cases of this partial kinking theory. The "square" yield criterion is obtained when $\mu = 1$ and Woods' result is obtained when $\mu = \sqrt{2}$. Thus μ has a value in the range 1 to 1.414. Wood refers to tests done by Hedley indicating that $\mu = 1.15$. Kiviecinski obtained a $\mu = 1.188$ from his tests. Thus it appears that though a slab may be isotropically reinforced, its ultimate moment capacity will be increased by about 18% for bending about an axis at 45° to the direction of reinforcement bars. This was the case in this series of tests, where the yield-lines were along the diagonals of the slabs. Allowing for these two considerations the theoretical value of W_u/m become $8 \times 1.5 \times 1.18 = 14.2$. Most of the results agree quite well with the value, though there are some considerably greater as shown in Table 4.1. This may be due to lateral restraint of the slabs by the clamping device used to ensure that the slabs were simply supported, which may have given rise to compressive membrane stresses.

4.4 Summary:

Though the simple yield-line theory underestimated the ultimate load of the slabs, refinements to take into account additional factors gives good agreement with theory. These factors are the improved strength characteristics of microconcrete not taken into account by ultimate load theory, and kinking of reinforcement across the yield lines. Some results were even higher than predicted by the modified theory, and this may have been due to compressive membrane stresses caused by the clamping device.

CHAPTER V

SPECIAL AND PILOT TESTS ON SLABS AND BEAMS
DYNAMIC TEST ON AGED CONCRETE SLAB

5.1 General

In this chapter an attempt to measure the dynamic deflections of a slab subjected to impact load is described. At the conclusion of the series of impact tests described in Chapter III one 25 mm slab remained untested and it was hoped that the strain at which concrete cracks in impact could be found from this test. A pilot study of steel-concrete-steel sandwich beams is also described in this chapter.

5.2 Impact Test

The same testing procedure was used as that described in 2.7. In order to measure the deflections a dial gauge was supported on a bar of length 750 mm directly attached to slab brackets mounting at the ends of the bar. This was to ensure that the deflection readings represent the actual vertical displacement of this slab, and not the deflection of the slab relative to some part of the testing rig. The plunger of the dial gauge was glued to the underside of the slab to eliminate overshoot. An attempt was made to measure the strain in the concrete using a strain gauge and portable strain meter, but this did not succeed. A number of measurewere taken for drops of 50, 75, and 100 mm. At drops greater than this dial gauge readings could not be made. Details of the slab and results of the impact test are given in Fig. II. 8.

5.3 Discussion of Results

In all cases the dynamic deflections in the uncracked range were lower than those obtained in Chapter III based on equations (4) and (5). These were calculated without using a Simms Reduction Factor. For beams the Simms Reduction Factor is

given by (using the notation of Chapter III) : $\alpha = \left(\frac{1}{1 + \frac{4}{5}\frac{W_b}{W_m}}\right)$

Applying it in this form to the slab in question, using $W_b = W_m$ we get

$$\alpha = 1/(1 + 4/5) = 0 \cdot 55$$

The energy equation in the uncracked range is

$$\alpha W_m (S + \delta) = \tfrac{1}{2} k \delta^2$$

U sing this equation the theoretical values of dynamic deflection are

MASS (kg)	DROP (mm)	MOMENTUM $_{-1}$ kg. m. sec	K kN/mm	DEFLECTION (mm)	EXPERIMENTAL DEFLECTION (mm)
33	50	32.7	13.3	1.2	1.0
33	75	40.0	10.0	1.7	1.35
33	100	46.2	10.0	1.9	1.40

The Simms Reduction Factor was obtained from impact tests on beams and is therefore not strictly applicable to slabs.

The use of a value of α in the region of 0.35 would have given a closer agreement with experiment.

The deflection at first crack from static tests on slabs of 25 mm thickness was of the order of 0.8 mm. In the impact test the deflection sustained without cracking was 1.4 mm. This gives the ratio dynamic cracking strain to static cracking strain of 1.75. This ratio is comparable to that found by other investigators. Watstein (1953) investigated the compressive strength of concrete subjected to varying rates of strain and obtained, at the highest rates, crushing strengths 1.8 times the static strength. Chung (1978) investigated the shear strength of concrete under dynamic loads and obtained values in the region of 1.75 to 2.02.

Static Tests on Composite Beams

5.4 General

The object of this investigation was to examine the feasibility of a steel-microconcrete composite with a view to imroving the strength of slabs. This is a pilot study to examine the effect of composite construction on simply supported beam specimens under static loading. A steel plate was attached to the tension flange by means of polymeric adhesive. The central deflection of the specimen was measured.

5.5 Specification

Micronconcrete:

The micronconcrete mix utilised was that reported in Chapter 11, Section 2.2 and the mixing procedure was also as described. Two layers of 25mm (1") square grid of 1.66mm diameter wire were used as internal reinforcement. Bottom cover of 5mm and spacing of 5mm was provided. The specimens were cast, cured and prepared for testing as before. A high quality finish was desirable for the successful use of the adhesive.

Steel:

A sheet of galvanised steel plate 1 mm thick was attached to the tension face of the microconcrete to act as additional tensile reinforcemnt.

Aluminium:

A plate of aluminium 1.5mm thick was attached to the compressive face of the microconcrete to prevent crushing under the load.

Preparation of composite:

The smooth face of the microconcrete specimen was chosen as the tensile face, it was then cleaned thoroughly with acetone. One face of the steel plate was also cleaned. The activator was painted onto both clean surfaces. The

adhesive was applied to the microconcrete surface and the steel plate was firmly clamped on the beam. The clamps were removed after 10 minutes. A similar procedure was used for the aluminium plate.

	Dimensions	
Microconcrete beam	Length	600mm
	width	75mm
	Depth	25mm
	span	450mm
Steel plate	Length	600mm
	width	75mm
	Thickness	1mm
Aluminium plate	Length	450mm
	width	75mm
	thickness	1.5mm

5.6 Testing Procedure

The tests were carried out in a Denison Universal testing machine. The load was applied in increments of 0.2 kilonewton at mid span and the central deflection recorded when stable deflection was attained i.e. initial creep included in measurement. The sides of the specimen were examined for crack development.

5.7 Test Results

The results of theflexural tests are shown in Figs. V.2,3. There is a marked difference between the two test results. The composite beam sustained at a considerably higher load than the control specimen. In both cases cracking in the concrete began along two lines on the tensile face, one either side of the centre line, the spacing between the cracks being greater for the non-plated specimen. As the microconcrete in the composite section began to crack the aluminium plate started to crimp, lifting some of the surface concrete with it. The tensile plate remained firmly fixed everywhere except in the central region where cracking of the concrete had occurred. With increasing load the steel plate began to extend. This creep was followed by strain hardening and the specimen finally failed by shearing along the steel-adhesive

interface on the tension side of the beam. The specimens at failure together with the details of the loading are shown in Fig. V2 and Fig. V.3.

5.8. Discussion of test results

One effect of the steel plate on the tensile face of the beam is to increase the depth of the neutral axis thus creating a larger area of compression concrete which can be utilised. The galvanised steel mesh was found to have little effect on the ultimate strength of the specimen but it does aid crack control. In both cases the specimens failed in a manner characteristic of under reinforced concrete sections. The tensile steel plate was able to resist the applied load after extensive cracking of the concrete had occurred. The bond failure between the steel and the adhesive indicates that shear failure did occur after strain hardening of the steel viz. an extension of 8mm in the steel plate in the central region was observed. The test on the steel-concrete sandwich plate indicates that flat mesh reinforcement could be omitted without loss of structural strength in flexure. Indeed the shear strength could be enhanced by inserting spiral reinforcement which would also act as a spacer for the metal cladding.

CHAPTER VI

CONCLUSIONS

6.1. General:

The following conclusion can be drawn from this research.

1. Initial cracking of the 40mm slabs occured when point loading reached values in the region 13 - 19 kN on simply supported slabs spanning 650mm.

2. Initial cracking of the 25mm slabs occured at a point load of 6 kN.

3. Good agreement between theoretical and experimental deflections were obtained for initial cracking loads.

4. The steel ratio (0.5 - 1.5%) had only slight effects on the initial cracking loads.

5. The theoretical stresses computed at first crack were rather high due to the concentrated load, indicating that the behaviour of the concrete slab was different from that of a thin plate under concentrated loads.

6. An allowable working stress of 7 N/mm^2 would insure that no detrimental cracking under static load would develop.

7. The experiments gave higher ultimate strengths than those calculated on the basis of Yield-Line theory. Experimental values exceeded theoretical by 50% in some tests.

8. Concrete slabs will sustain higher deflections at first crack due to impact load than due to static loads.

9. The 25mm slabs cdacked when the momentum of the striker was 46 kg. m. sec^{-1}

10. The 40 mm slabs cracked when the momentum of the striker reached 75 kg. m. s^{-1}

11. The ratio of dynamic to static cracking strain in the concrete appears to be of the order of 1.75.

12. Although, strictly speaking not formulated for slabs, the use of the Simms Reduction Factor in its original form leads to overestimation of dynamic deflections.

13. The tests on the composite beam showed that the steel plate and concrete beam could be successfully bonded together. Failure occured in a manner characteristic of under-reinforced concrete sections at a load approximately ten times as great as for the unclad sections.

6.2 Areas for Future Research

Further research into the properties and behaviour of composite sections is envisaged. In particular the impact resistance of these sections, and the effect of environmental factors such as temperature on the adhesive bond need further study.

REFERENCES

1. ROARKE & YOUNG (1975) Formulas for Stress and Strain
   McGraw-Hill New York.

2. CRACKNESS, C.J. AND JARMAN, D.A. "Effect of Heavy Impact Loads on Structural Members"
   Concrete, September 1973 pp. 49 - 50.

3. SIMMS, J. G. "Actual and Estimated impact resistance of some Reinforced Concrete Units Failing in Bending",
   Journal of the Institute of Civil Engineers, No. 4 1944-45 February 1945.

4. MANSFIELD, E.H. "Studies in Collapse Analysis of Rigid-Plastic Plates with a Square Yield Diagram",
   Proceedings of the Royal Society (A) Vol. 241 1957 pp. 311.

5. GLYNN, T.E. AND AL-SALIHI, M.Z. "Tensile Strength of Reinforced Microconcrete"
   FINAL TECHNICAL REPORT to EUROPEAN RESEARCH OFFICE August 1975

6. WOOD, R.H. "Plastic and Elastic Design of Slabs and Plates"
   London, Thames and Hudson, 1961, pp. 344.

7. KWIECINSKI, M.W. "Yield Criterion for Initially Isotropically Reinforced Slab",
   Magazine of Concrete Research Vol. 17, No. 51 June, 1965 pp. 97 - 100.

8. KWIECINSKI, M.W. "Some Tests on the Yield Criterion for a Reinforced Concrete Slab",
Magazine of Concrete Research, Vol. 17, No. 52, September 1965 pp. 135 - 138.

9. WATSTEIN, D. "Effect of Straining Rate on the Compressive Strength and Elastic Properties of Concrete".
Journal of the American Concrete Institute. Vol. 24, No. 8, April, 1953, pp. 729 - 744.

10. TAYLOR R., MAHER B.R.H., HAYES B. "Effect of Arrangement of Reinforcement on the Behaviour of Reinforced Concrete Slabs",
Magazine of Concrete Research Vol. 18 No. 55, June 1966, pp. 852 - 894.

11. CHUNG, H.W. "Shear Strength of Concrete Joints under Dynamic Load".
Concrete, March 1978, P. P. 27 - 29

BIBLIOGRAPHY

1. SHAH, S. P., KEY JN., W.H. "Impact Resistance of Ferrocement" Tour ASCE STRUCTURAL DIV. January 1972 pp. 111, 123

2. JOHNSTON C.D., MOWAT D.N. 'Ferrocement Material Behaviour in Flexure' Tour of ASCE Structural DIV October 1974 pp. 2053 2069

3. SOLOMON, S.K., SMITH, D.W. AND CUSENS, A.R. "Flexural Tests of Steel - Concrete - Steel Sandwiches". Magazine of Concrete Research, Vol. 28, No. 94, March 1976 p.p. 13 - 20.

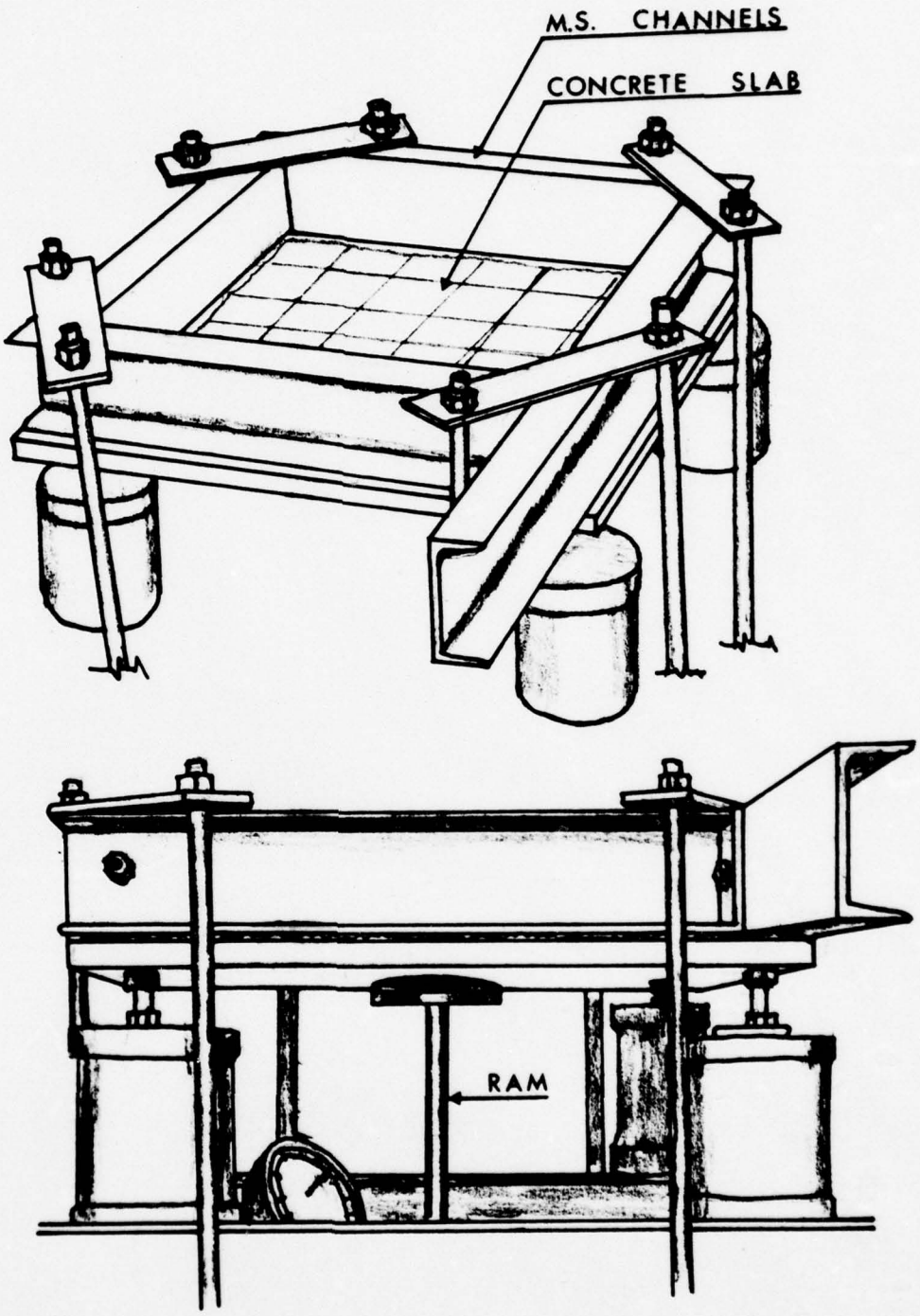

FIG II.1 LAYOUT OF STATIC TESTS.

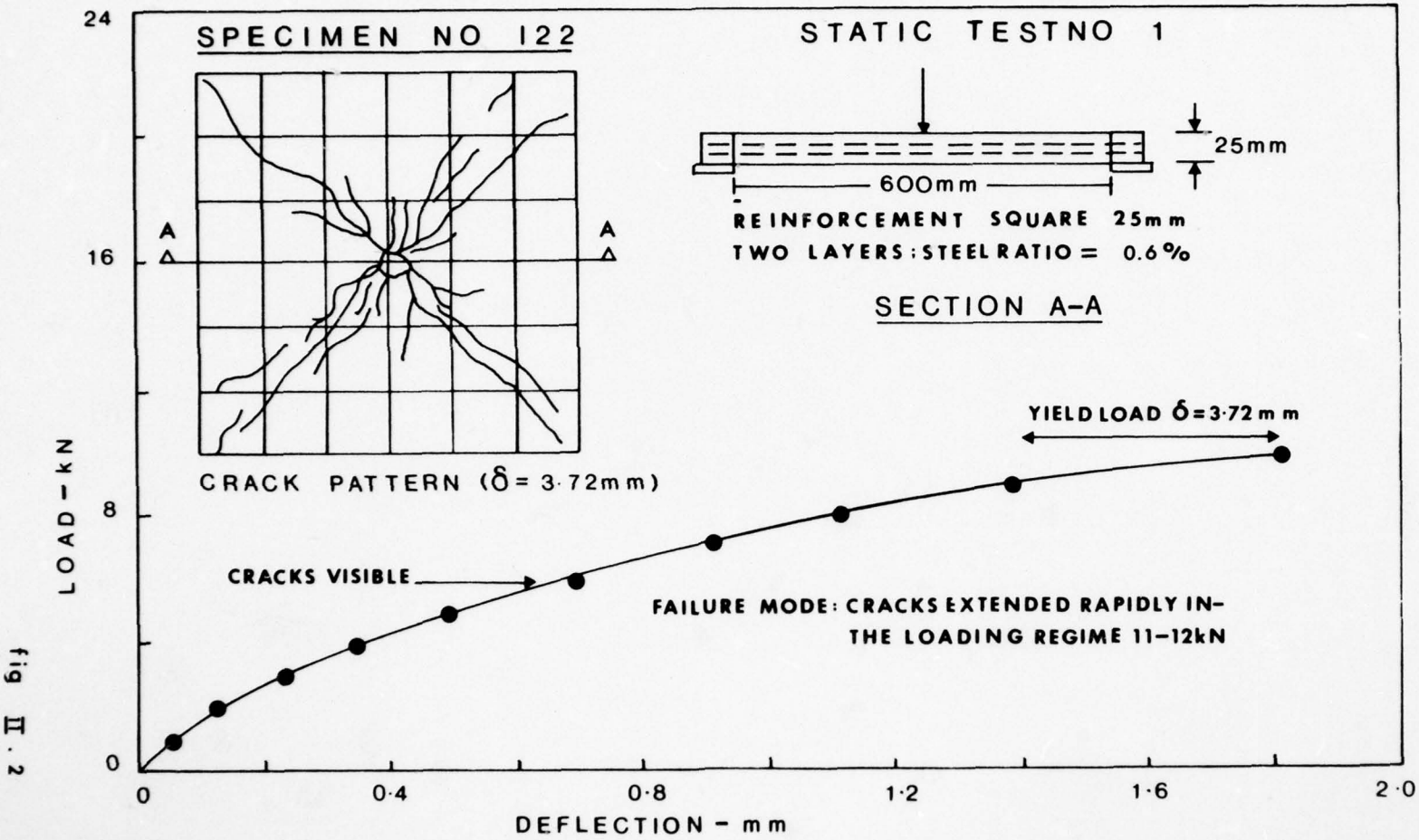
SPECIMEN NO 122
STATIC TESTNO 1
25mm
600mm
REINFORCEMENT SQUARE 25mm
TWO LAYERS : STEEL RATIO = 0.6%
SECTION A–A
A
A
CRACK PATTERN (δ = 3·72mm)
YIELD LOAD δ = 3·72 mm
CRACKS VISIBLE
FAILURE MODE: CRACKS EXTENDED RAPIDLY IN-
THE LOADING REGIME 11–12kN
LOAD – kN
24
16
8
0
0
0·4
0·8
1·2
1·6
2·0
DEFLECTION – mm

fig II.2

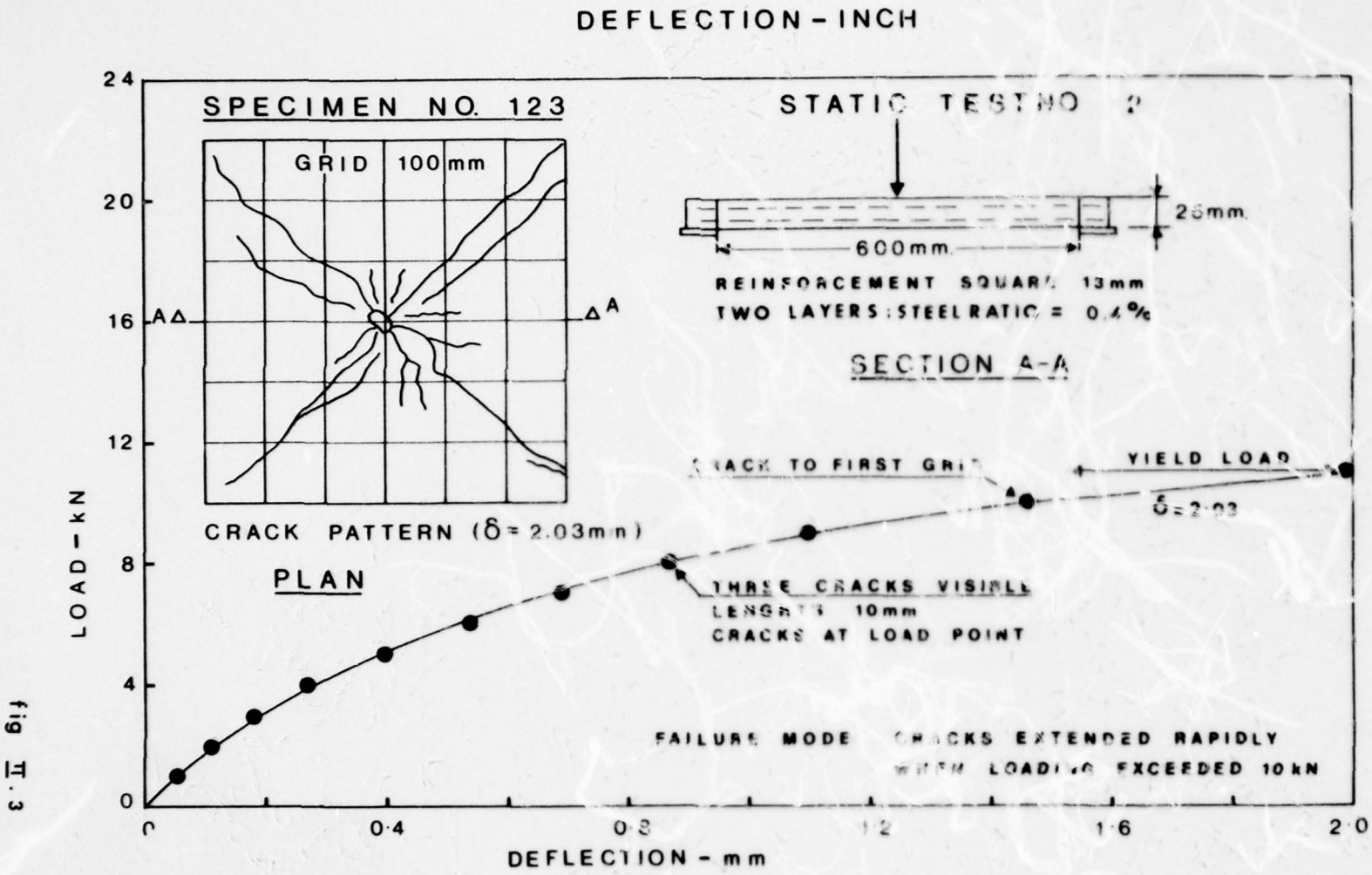
DEFLECTION - INCH
SPECIMEN NO. 123
GRID 100mm
A
A
A
A
CRACK PATTERN (δ = 2.03mm)
PLAN
STATIC TEST NO 2
25mm
600mm
REINFORCEMENT SQUARE 13mm
TWO LAYERS : STEEL RATIO = 0.4%
SECTION A-A
CRACK TO FIRST GRID
YIELD LOAD
δ = 2.03
THREE CRACKS VISIBLE
LENGTH 10mm
CRACKS AT LOAD POINT
FAILURE MODE CRACKS EXTENDED RAPIDLY
WHEN LOADING EXCEEDED 10 kN
LOAD - kN
DEFLECTION - mm
0
4
8
12
16
20
24
0·4
0·8
1·2
1·6
2·0

fig II.3

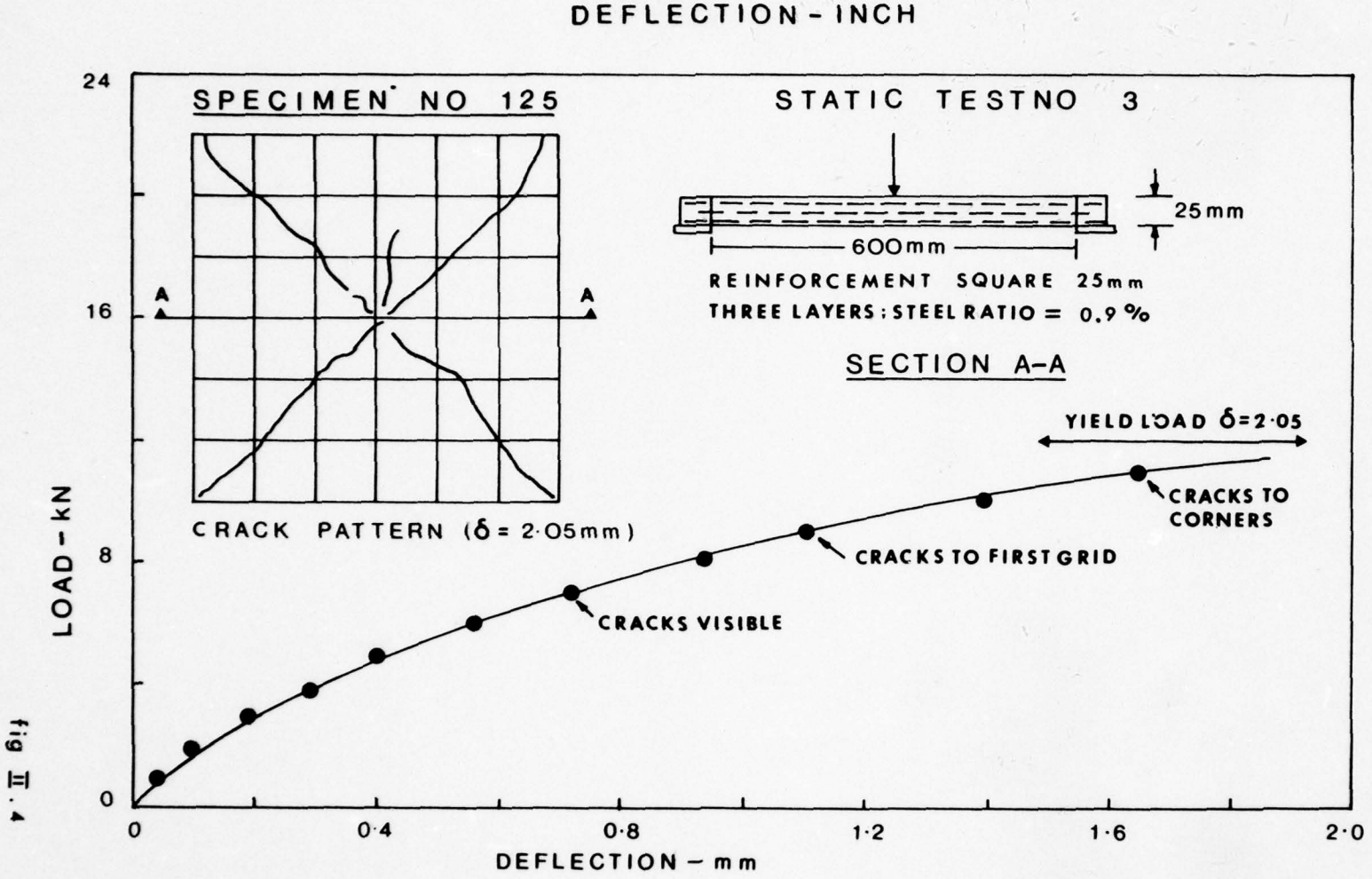
DEFLECTION - INCH
SPECIMEN NO 125
STATIC TESTNO 3
25mm
600mm
REINFORCEMENT SQUARE 25mm
THREE LAYERS : STEEL RATIO = 0.9 %
SECTION A–A
A
A
CRACK PATTERN (δ = 2·05mm)
YIELD LOAD δ=2·05
CRACKS TO CORNERS
CRACKS TO FIRST GRID
CRACKS VISIBLE
LOAD - kN
24
16
8
0
0
0·4
0·8
1·2
1·6
2·0
DEFLECTION – mm

Fig III.4

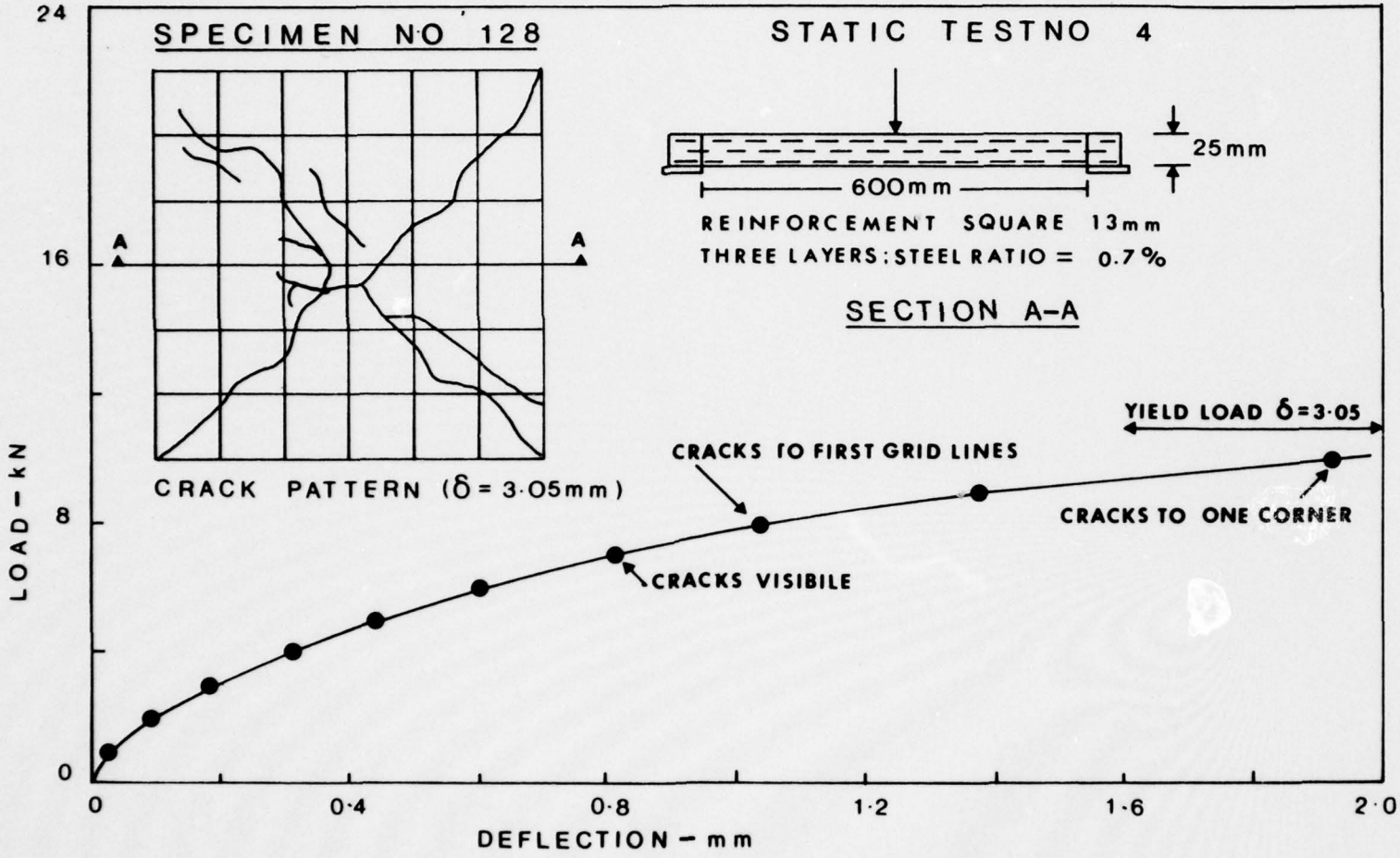
SPECIMEN NO 128
STATIC TESTNO 4
25mm
600mm
REINFORCEMENT SQUARE 13mm
THREE LAYERS: STEEL RATIO = 0.7%
SECTION A-A
A
A
CRACK PATTERN (δ = 3·05mm)
YIELD LOAD δ=3·05
CRACKS TO FIRST GRID LINES
CRACKS TO ONE CORNER
CRACKS VISIBILE
LOAD - kN
DEFLECTION - mm
24
16
8
0
0
0·4
0·8
1·2
1·6
2·0

fig II.5

TEST NO. 14

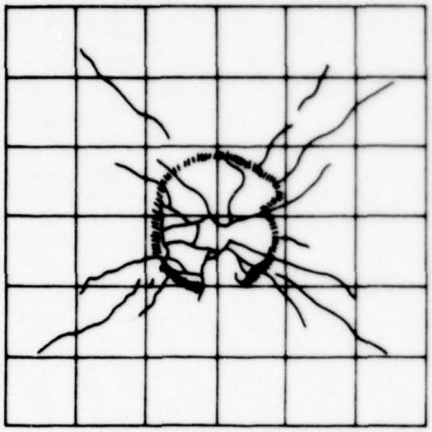

CRACK PATTERN

REINFORCEMENT : TWO LAYERS OF SQUARE MESH – 25mm
STEEL RATIO : 0.6 %
WEIGHT OF SLAB : 31.5 kg
WEIGHT OF IMPACTOR : 33kg

FREE DROP (mm)	REMARKS – CRACKING MODE
25	NO CRACKS VISIBLE
50	"
75	"
100	SHORT CRACKS AT CENTRE
125	CRACKS PROPAGATED
150	CRACKS TO FIRST GRID
175	
200	PUNCHING SHEAR CRACKS
225	CRACKS AS SKETCHED

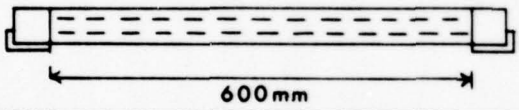

SPECIMEN NO 121

TEST NO 15

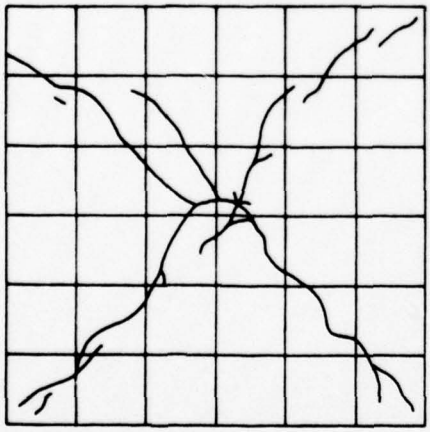

PLAN (TENSION FACE AT FAILURE)

REINFORCEMENT : TWO LAYERS OF SQUARE MESH – 13mm
STEEL RATIO : 0.4 %
WEIGHT OF SLAB : 31.5kg
WEIGHT OF IMPACTOR : 33kg

FREE DROP (mm)	REMARKS – CRACKING MODE
25	NO CRACKS VISIBLE
50	"
75	"
100	CRACK 15mm LONG (CENTRE)
125	CRACKS PROPOGATED
150	CRACK TO SECOND GRID LINES
175	CRACKS PROPAGATED TO COPNERS AS SHOWN

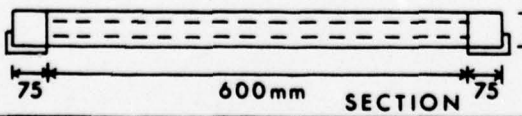

SECTION

SPECIMEN NO 124

IMPACT TEST DATA

FIG II.6

TEST NO. 16

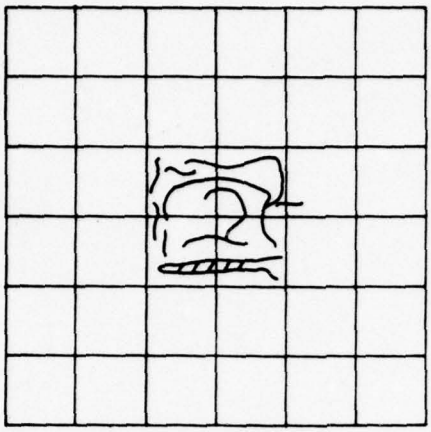

CRACK PATTERN

REINFORCEMENT: THREE LAYERS OF SQUARE MESH – 25mm
STEEL RATIO: 0.9 %
WEIGHT OF SLAB: 32.9 kg
WEIGHT OF IMPACTOR: 33kg

DROP mm	REMARKS
25	NO CRACKS VISIBLE
50	"
75	"
100	CIRCULAR CRACKS
125	CRACKS IN TWO GRIDS
150	CRACKS WITHIN FIRST GRIDS
175	CRACK PROPAGATED
200	CIRCULAR CRACKS DIAM 150mm
225	PUNCHING SHEAR FAILURE

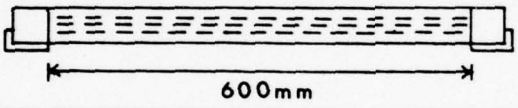

SPECIMEN NO 126

TEST NO. 17

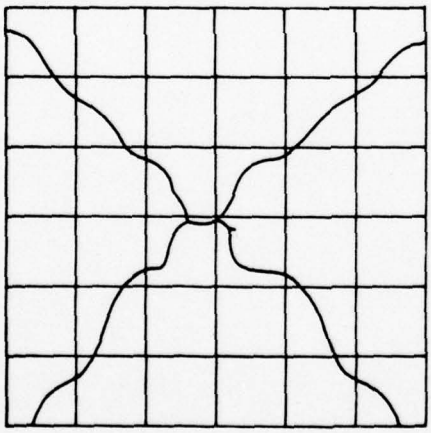

CRACK PATTERN

REINFORCEMENT: THREE LAYERS OF SQUARE MESH – 13mm
STEEL RATIO: 0.7 %
WEIGHT OF SLAB: 32.9kg
WEIGHT OF IMPACTOR: 33 kg

DROP mm	REMARKS
25	NO CRACKS VISIBLE
50	"
75	"
100	CRACK 15mm CENTRE
125	CRACKS TO FIRST GRID LINES
150	CRACK TO CORNERS IN TWO QUADRANTS
175	CRACK TO FOUR CORNERS AS SHOWN

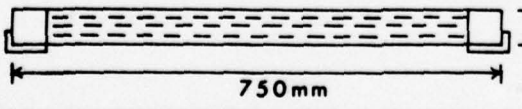

SPECIMEN NO 127

IMPACT TEST DATA

FIG II.7

TEST NO. 18

FREE DROP (m m)	REMARKS – CRACKING MODE	DEFLECTION (m m)
50	NO CRACKS VISIBLE	1.0
75	"	1.35
100	SMALL CRACK AT CENTRE	1.40
125	CRACK PROPAGATED	–
150	"	–
200	CRACKS TO EDGES	–
250	SPALLING AT CR.	–

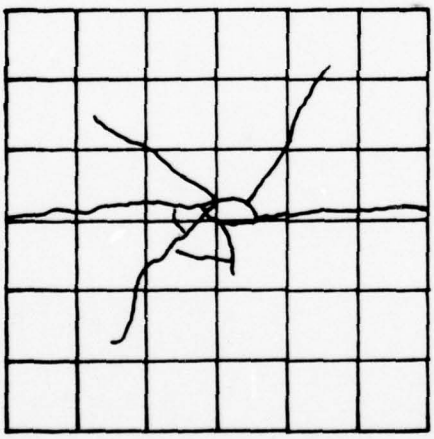

PLAN (TENSION FACE)

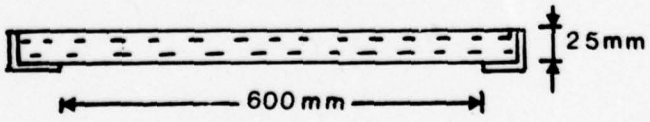

SECTION

REINFORCEMENT: TWO LAYERS OF SQUARE MESH – 13 m m

STEEL RATIO : 0.4 %

WEIGHT OF SLAB: 31.5 kg

WEIGHT OF IMPACTOR : 33 kg

SPECIAL IMPACT TEST

IMPACT TEST DATA

FIG II.8

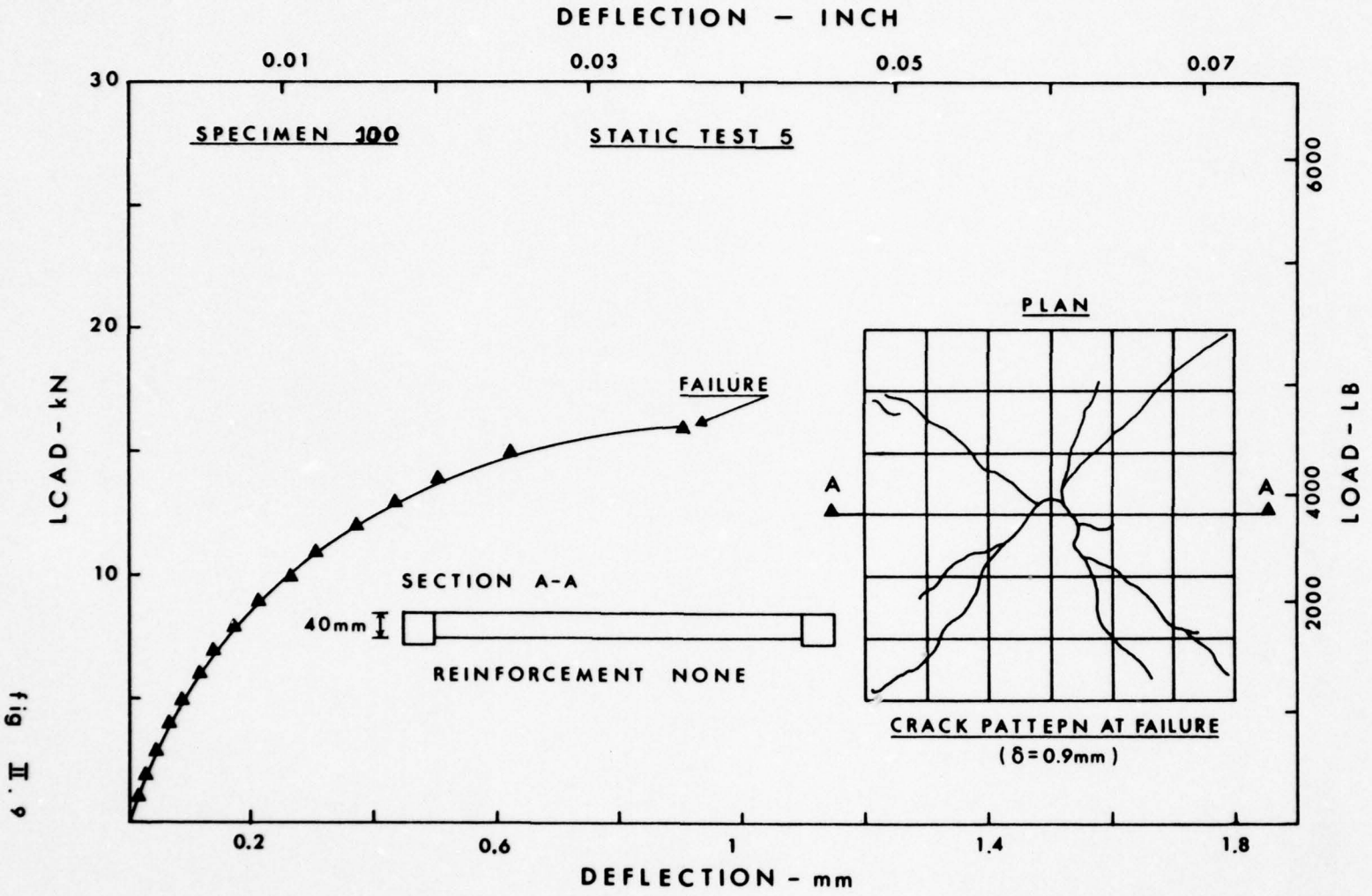

fig II.9

MID-SPAN DEFLECTION-VS-CENTRAL CONCENTRATED LOAD

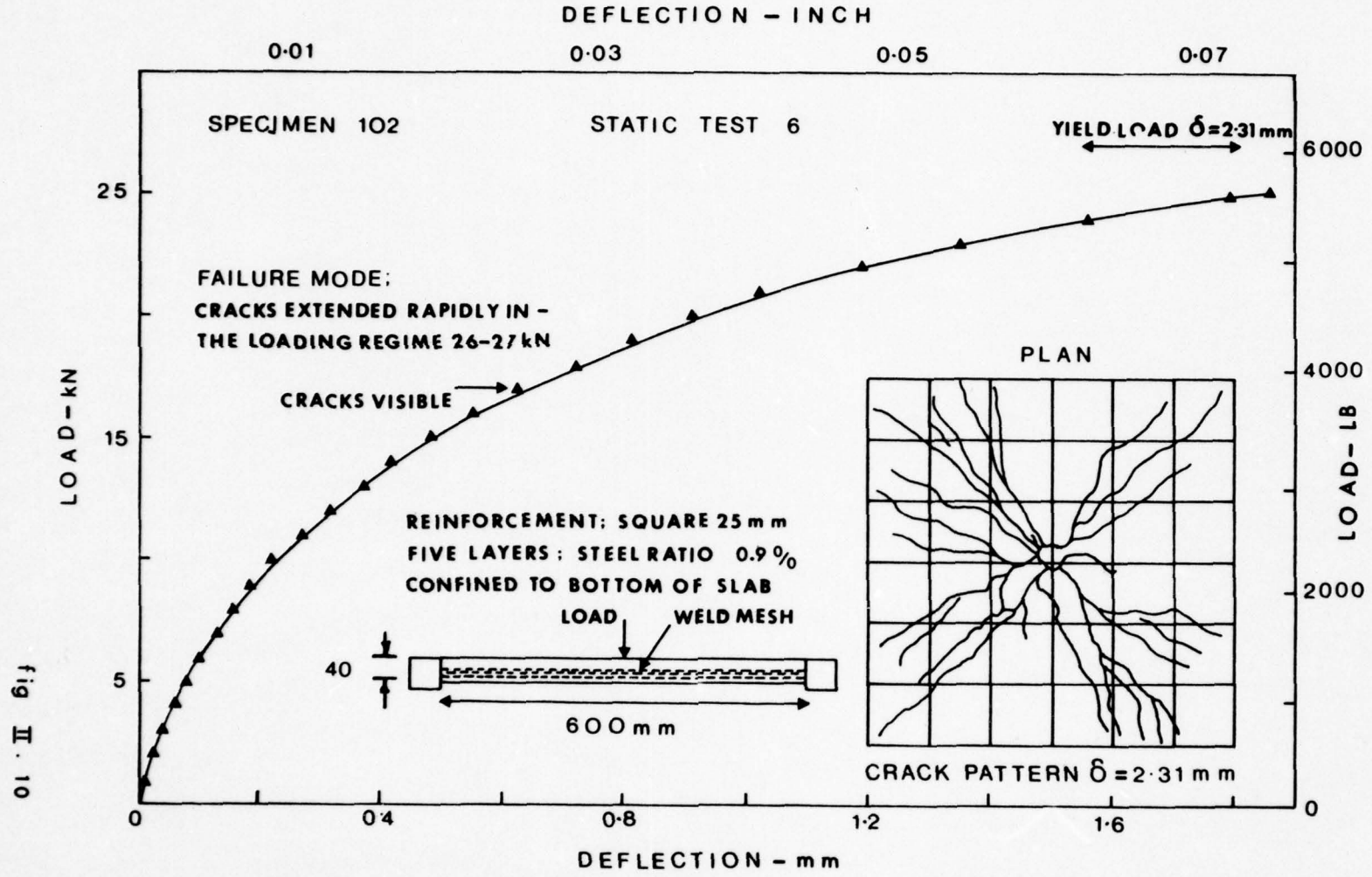

Fig II · 10

MID-SPAN DEFLECTION – VS – CENTRAL CONCENTRATED LOAD

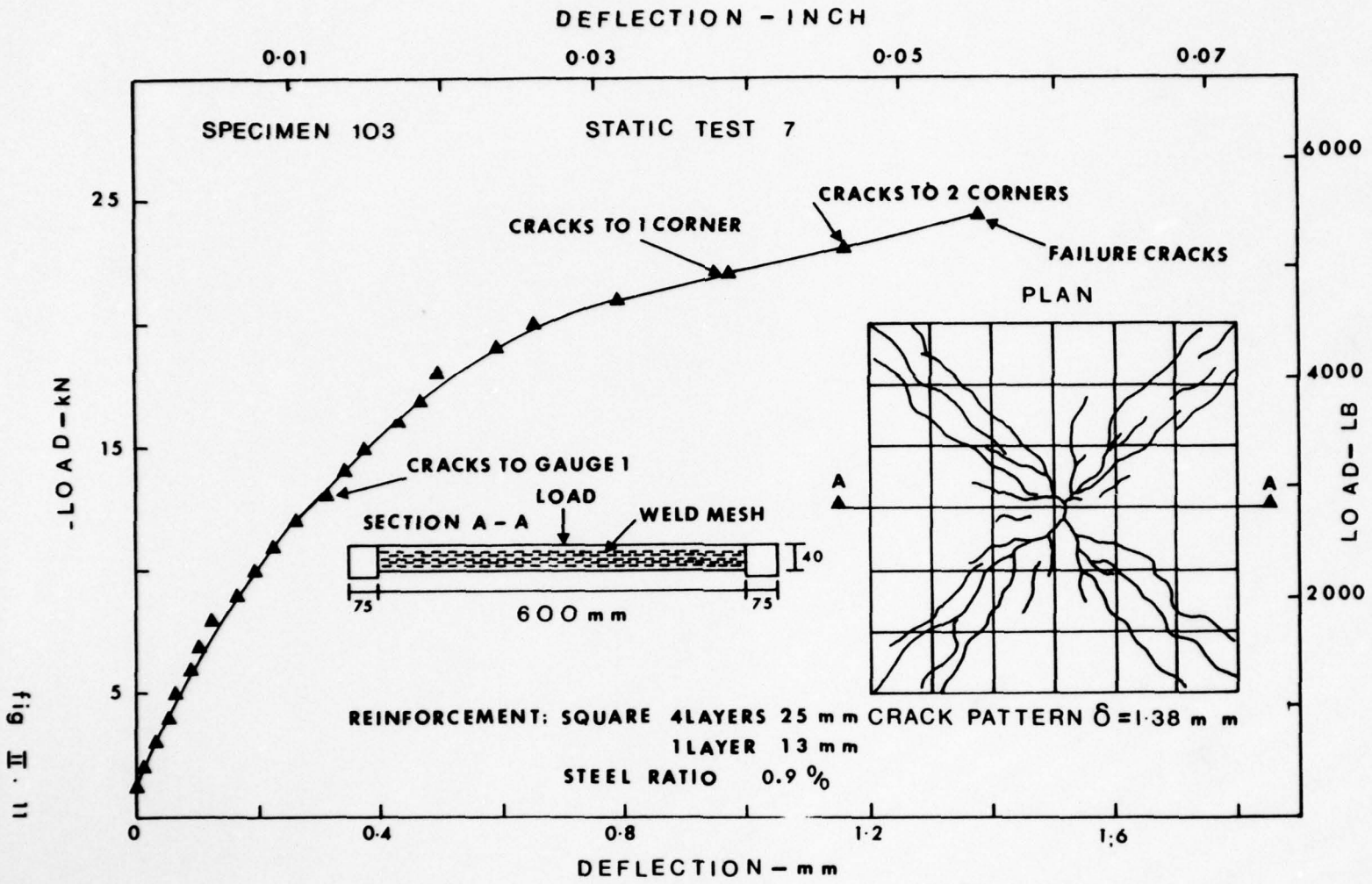

fig II · 11

MID-SPAN DEFLECTION - VS - CENTRAL CONCENTRATED LOAD

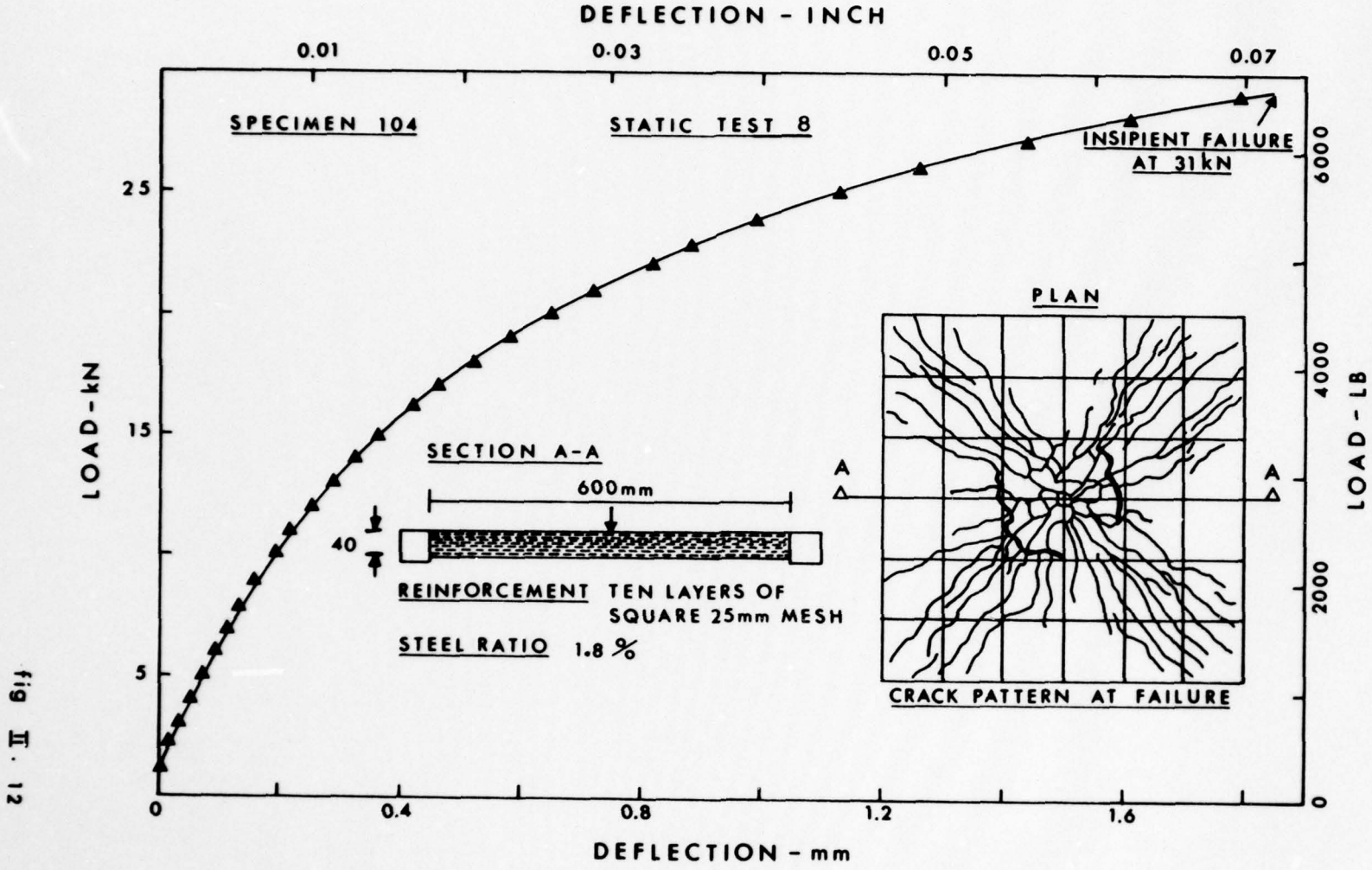

MID-SPAN DEFLECTION - VS - CENTRAL CONCENTRATED LOAD

fig II . 12

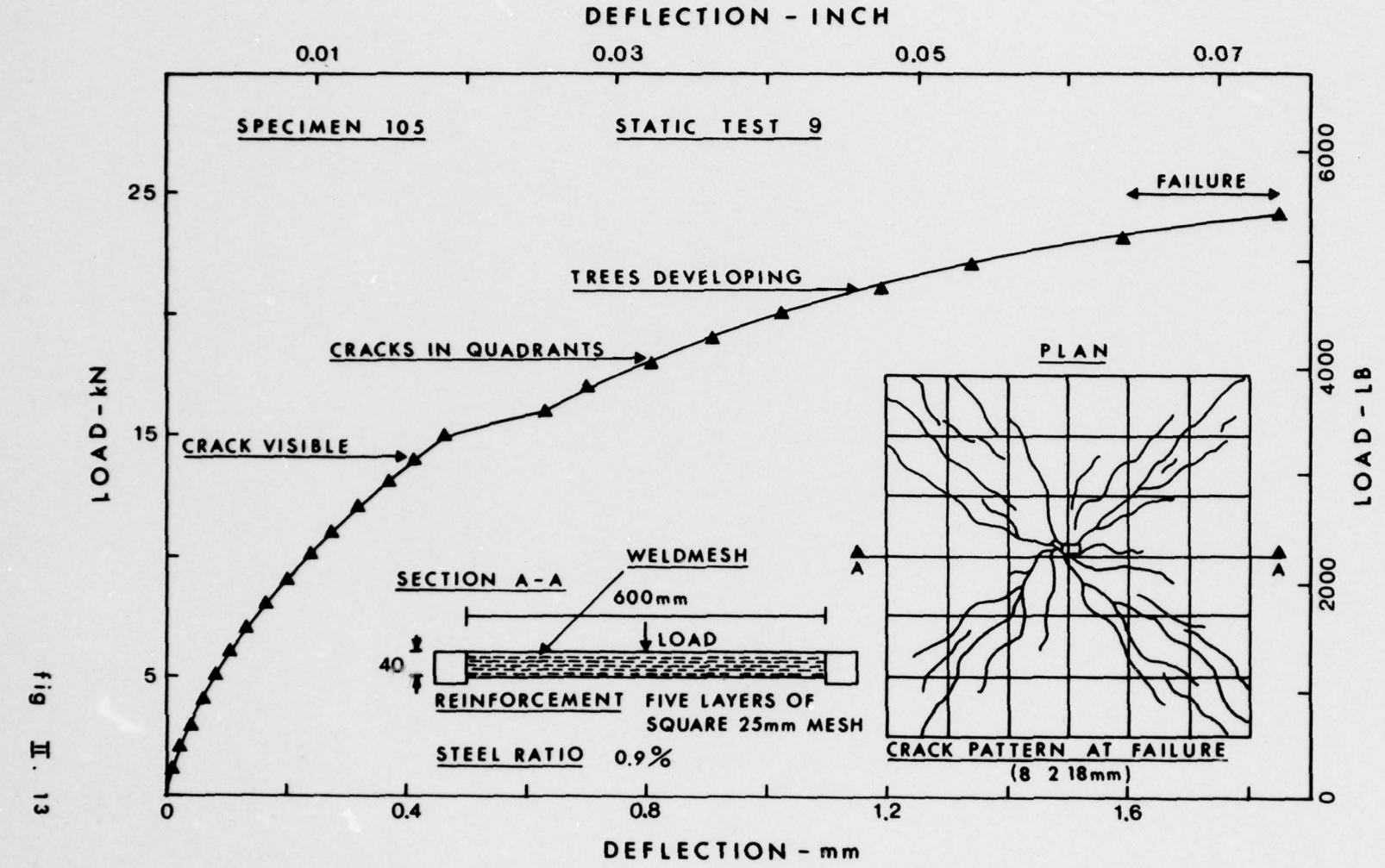

fig II. 13

MID-SPAN DEFLECTION - VS - CENTRAL CONCENTRATED LOAD

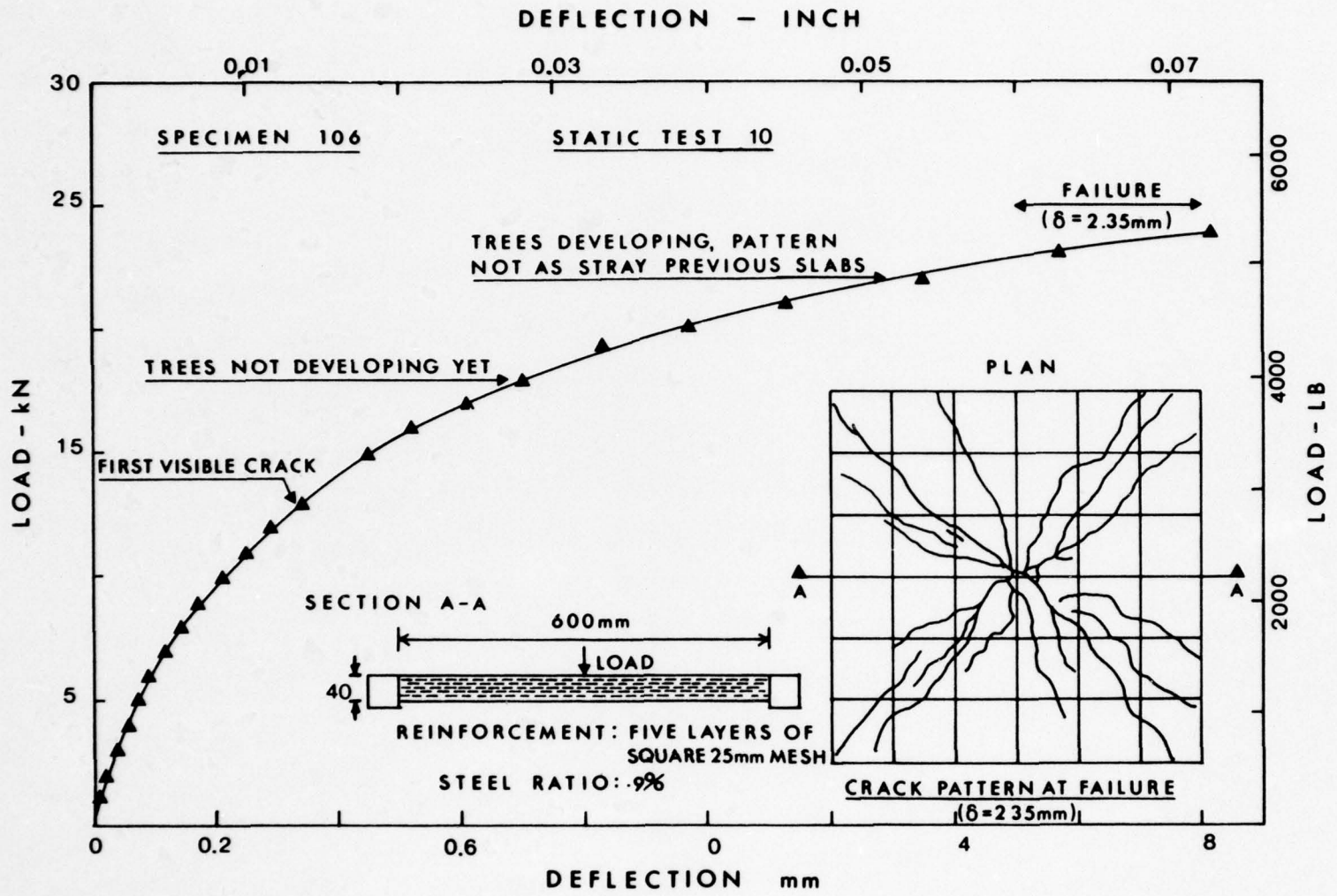

MID-SPAN DEFLECTION-VS-CENTRAL CONCENTRATED LOAD

fig II . 14

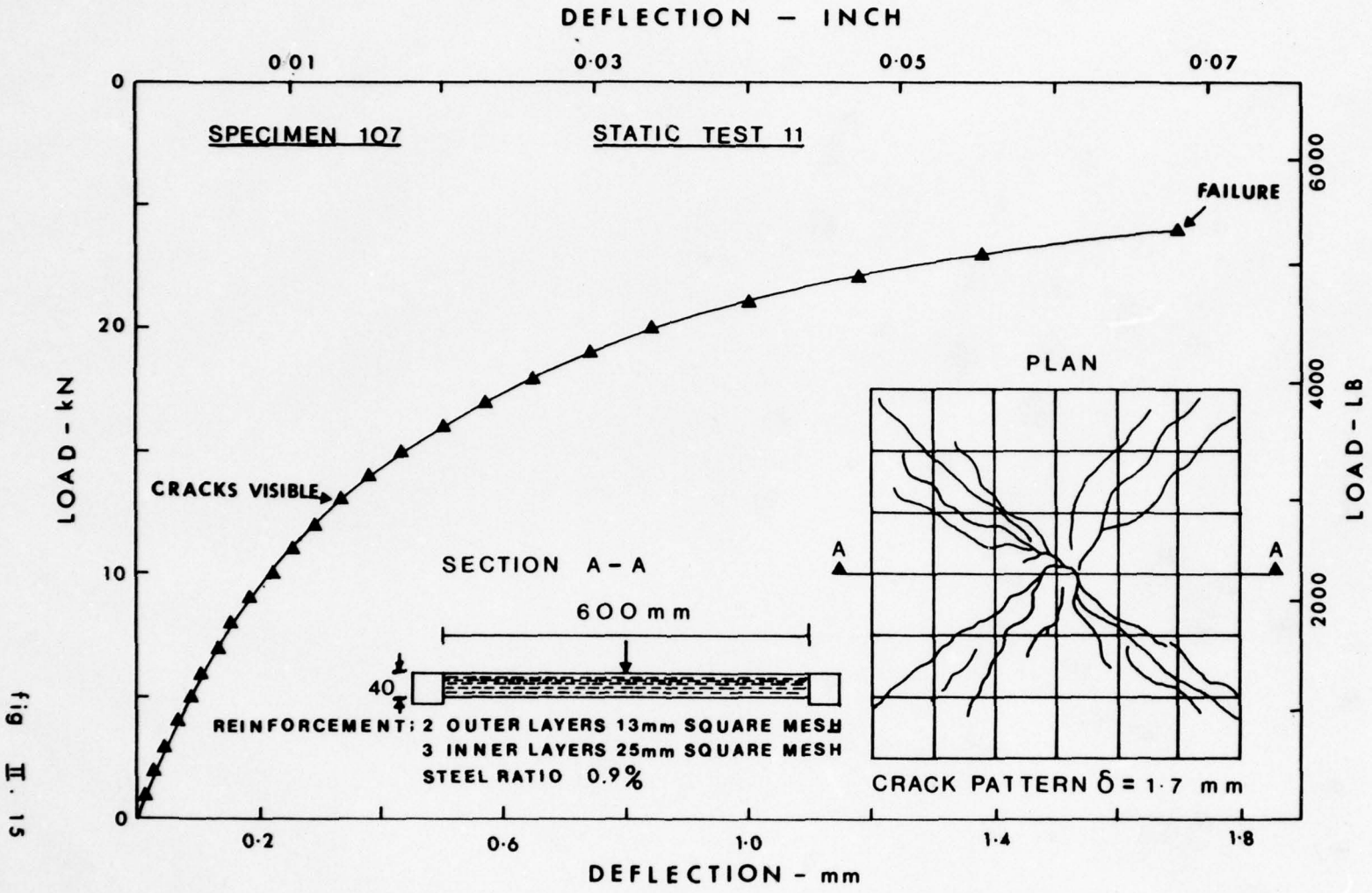

fig II·15

MID-SPAN DEFLECTION-VS-CENTRAL CONCENTRATED LOAD

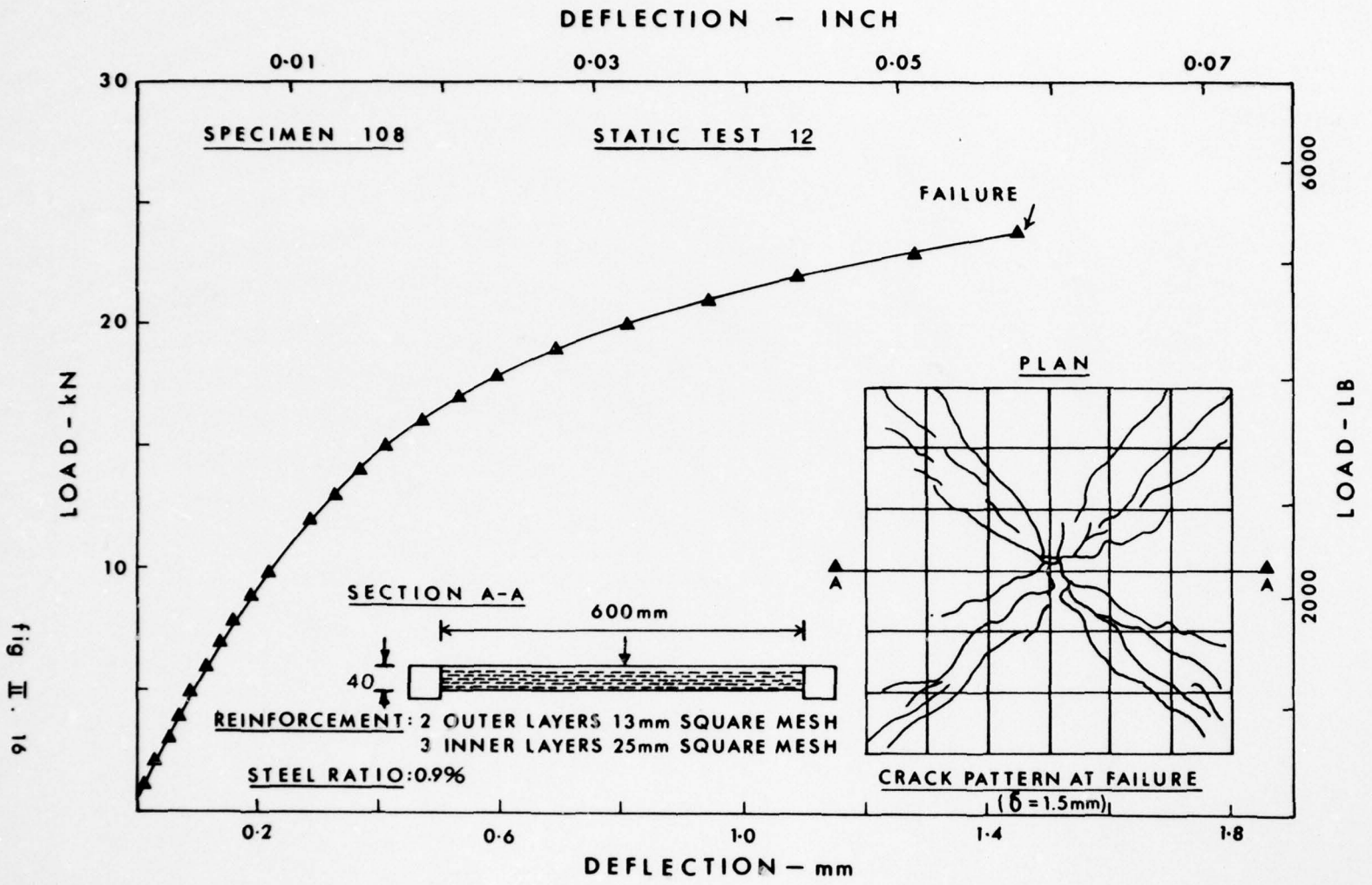

Fig II · 16

MID-SPAN DEFLECTION-VS-CENTRAL CONCENTRATED LOAD

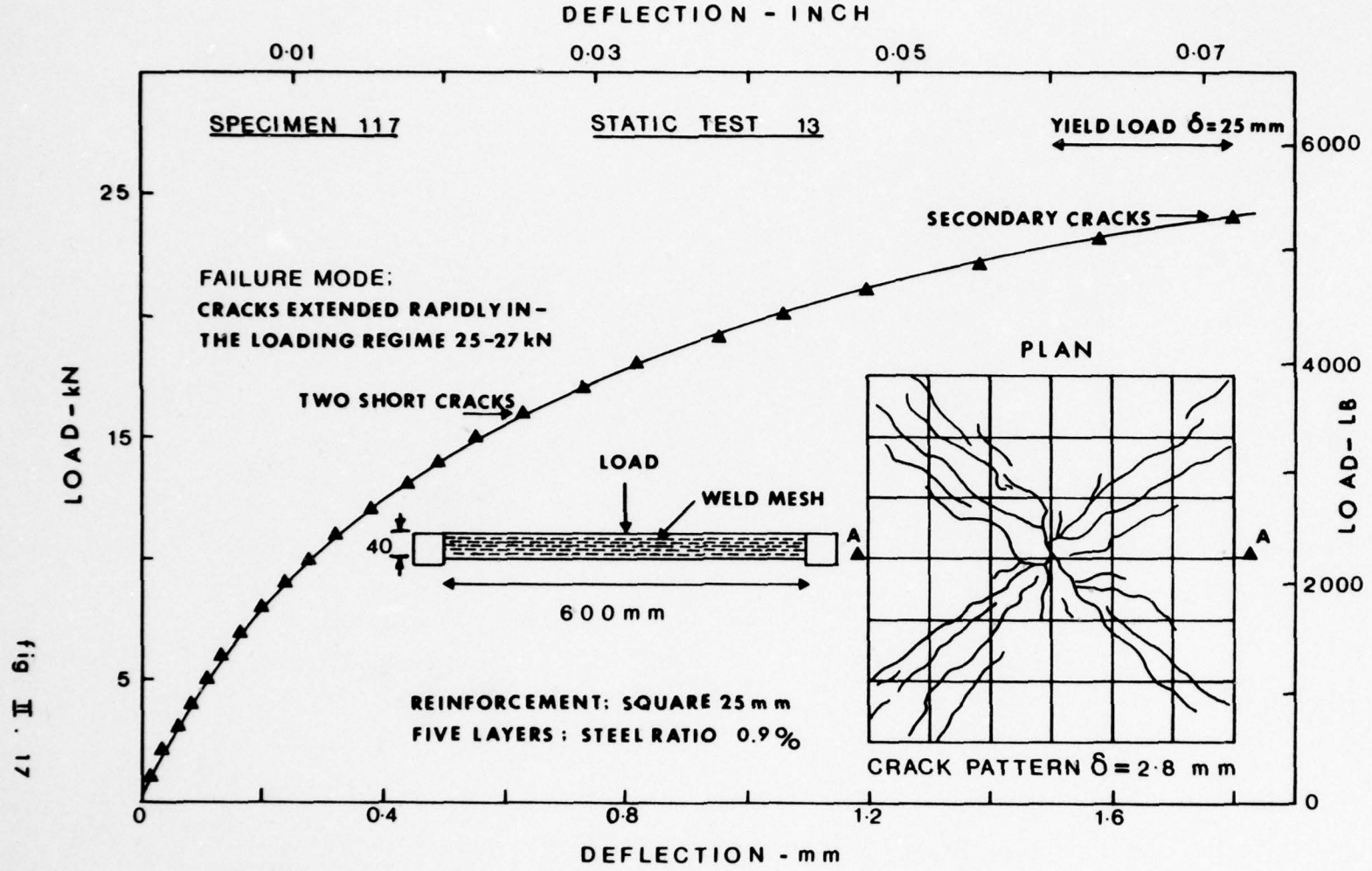

fig II . 17

MID-SPAN DEFLECTION -VS- CENTRAL CONCENTRATED LOAD

TEST NO 19

TRIAL

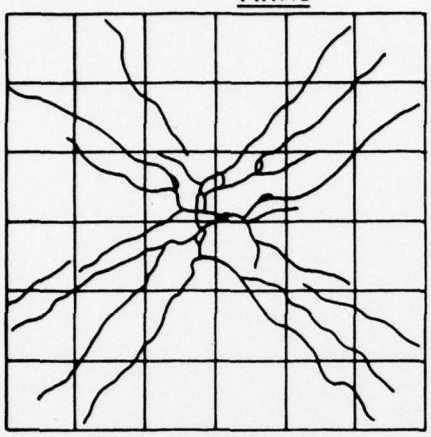

FINAL CRACK PATTERN

REINFORCEMENT: FIVE LAYERS OF SQUARE MESH
STEEL RATIO : 0.9 %
WEIGHT OF SLAB : 47.3kg
WEIGHT OF IMPACTOR : 47.8kg

FREE DROP (mm)	REMARKS – CRACKING MODE
25	NO CRACKS VISIBLE
50	"
75	"
100	"
125	"
150	VISIBLE CRACKS AT CENTRE
200	CRACKS TO FIRST GRID
250	RADIAL YIELD LINES DEVELOPING
275	NUMEROUS SECONDARY YIELD LINES
300	CRACKS TO ALL FOUR CORNERS

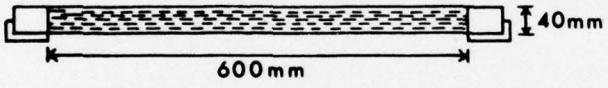

SPECIMEN NO 111

TEST NO 20

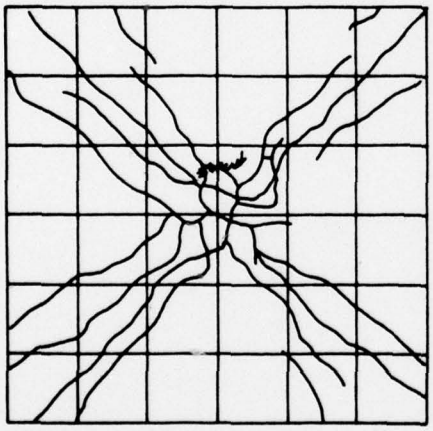

FINAL CRACK PATTERN

REINFORCEMENT : FIVE LAYERS OF SQUARE MESH – 25mm
STEEL RATIO : 0.9 %
WEIGHT OF SLAB : 47.3kg
WEIGHT OF IMPACTOR : 47.8kg

FREE DROP (mm)	REMARKS CRACKING MODE
25	NO CRACKS VISIBLE
50	"
75	"
100	"
125	SMALL CRACK VISIBLE
150	SHORT FINE CRACKS
175	CRACKS PROPAGATED
200	CRACKS TO FIRST GRID
225	CRACKS MID-WAY TO SECOND GRID
250	– LOAD SLIPPED –
275	YIELD LINES TO SECOND GRID
300	YIELD LINES TO ALL CORNERS

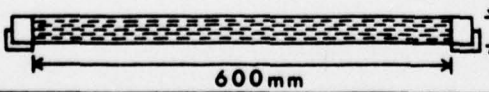

SPECIMEM NO 112

IMPACT TEST DATA

FIG II . 18

TEST NO 21

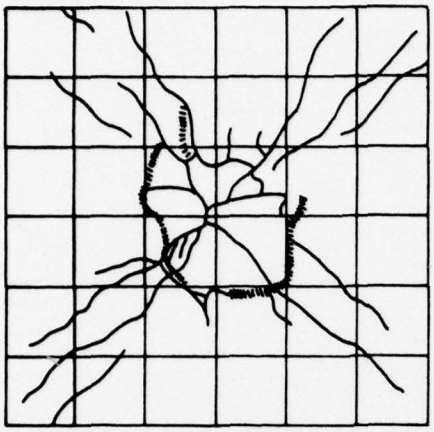

FINAL CRACK PATTERN

REINFORCEMENT : FIVE LAYERS OF SQUARE MESH – 25mm
STEEL RATIO : 0.94 %
WEIGHT OF SLAB : 47.3kg
WEIGHT OF IMPACTOR : 47.8kg

FR E DROP (mm)	REMARKS – CRACKING MODE
25	NO CRACKS VISIBLE
50	"
75	"
100	"
125	40mm
150	CRACK PROPAGATED BRANCHING
175	CRACKS BEYOND FIRST GRID
200	TWO CRACKS APPROACHING EDGES
225	TWO CRACKS TO EDGES
250	FAILURE ALSO PUNCHING SHEAR

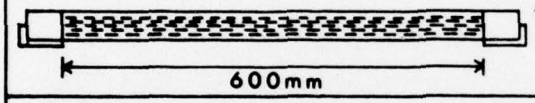

SPECIMEN NO 113

TEST NO 22

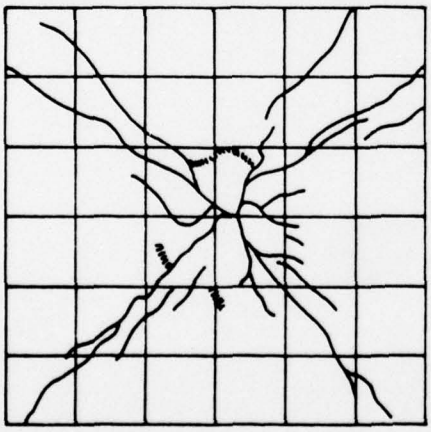

FINAL CRACK PATTERN

REINFORCEMENT : FIVE LAYERS OF SQUARE MESH – 25mm
STEEL RATIO : 0.94 %
WEIGHT OF SLAB : 47.3kg
WEIGHT OF IMPACTOR : 47.8kg

FREE DROP	REMARKS – CRACKING MODE
25	NO CRACKS VISIBLE
50	"
75	"
100	"
125	TWO SMALL CRACKS AT CENTRE
150	CRACKS PROPAGATED (REBOUND)
170	ONE CRACK TO FIRST GRID
200	CRACKS APPROACH SECOND GRID
225	NON UNIFORM CRACK PROPAGATION
250	FAILURE NO HONEYCOMBING

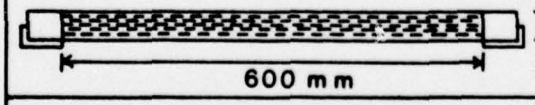

SPECIMEN NO 114

IMPACT TEST DATA

FIG II. 19

TEST NO. 23

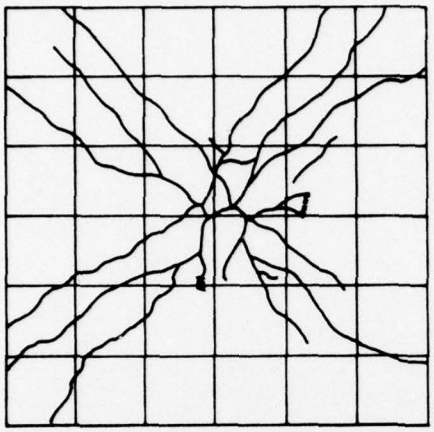

FINAL CRACK PATTERN

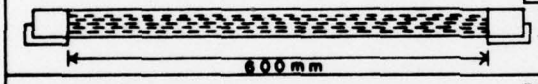

REINFORCEMENT : FIVE LAYERS OF SQUARE MESH – 25mm
STEEL RATIO 0.9 %
WEIGHT OF SLAB 47.3 kg
WEIGHT OF IMPACTOR 47.8 kg

FREE DROP (mm)	REMARKS – CRACKING MODE
25	NO CRACKS VISIBLE
50	
75	
100	SMALL CRACK NEAR CENTRE
125	CRACK SPREADING DIAGONALLY
150	CRACK HALF WAY TO FIRST GRID
175	CRACKS APPROACH FIRST GRID
200	CRACKS PAST FIRST GRID
225	CRACKS PROPAGATED
250	YIELD LINES TO THREE EDGES
275	PUNCHING AT CENTRE

SPECIMEN NO 115

TEST NO. 24

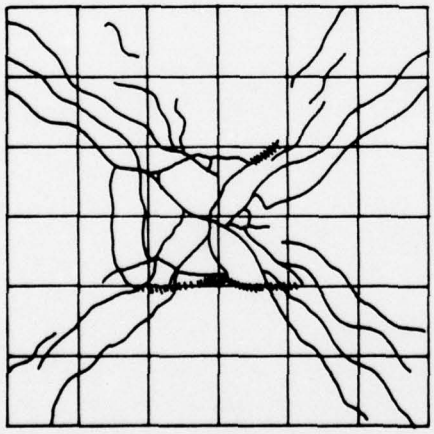

FINAL CRACK PATTERN

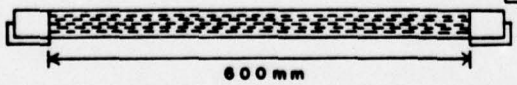

REINFORCEMENT : FIVE LAYERS OF SQUARE MESH – 25mm
STEEL RATIO 0.9 %
WEIGHT OF SLAB 47.3 kg
WEIGHT OF IMPACTOR 47.8 kg

FREE DROP (mm)	REMARKS – CRACKING MODE
50	NO VISIBLE EFFECTS
100	
150	TWO CRACKS ALONG GRID LINES
200	FOUR CRACKS TOWARDS FIRST GRID
225	ALL CRACKS BEYOND FIRST GRID
250	SECONDARY CRACKS, HONEYCOMBING
275	CRACKS PROPAGATED
300	CRACK DEVELOPMENT, NO EXTENTION
325	TWO CRACKS TO CORNERS
350	FAILURE, ALSO HONEYCOMBING

SPECIMEN NO 116

IMPACT TEST DATA

FIG II . 20

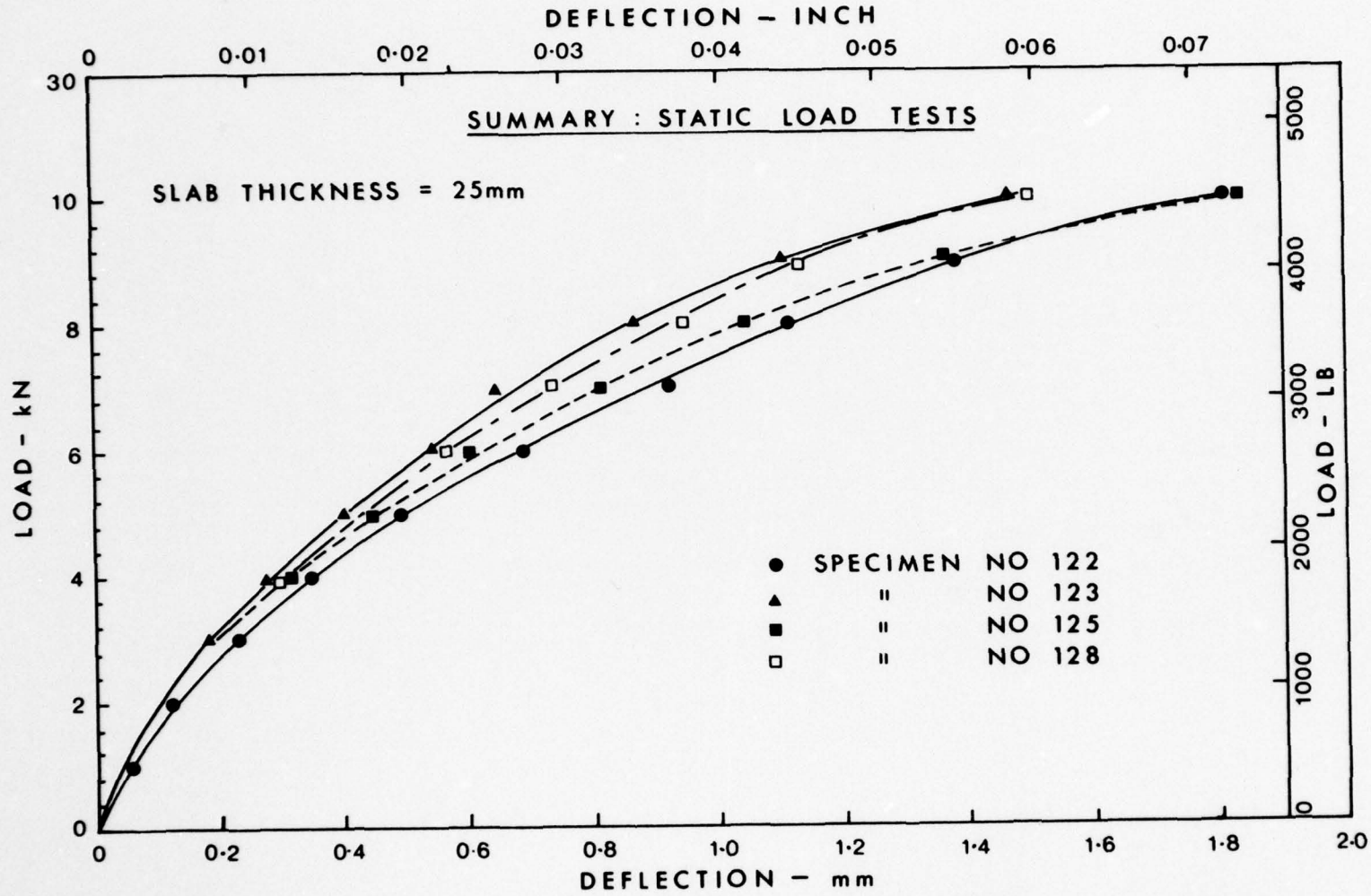

MID SPAN DEFLECTION - VS - CENTRAL CONCENTRATED LOAD

fig III.1

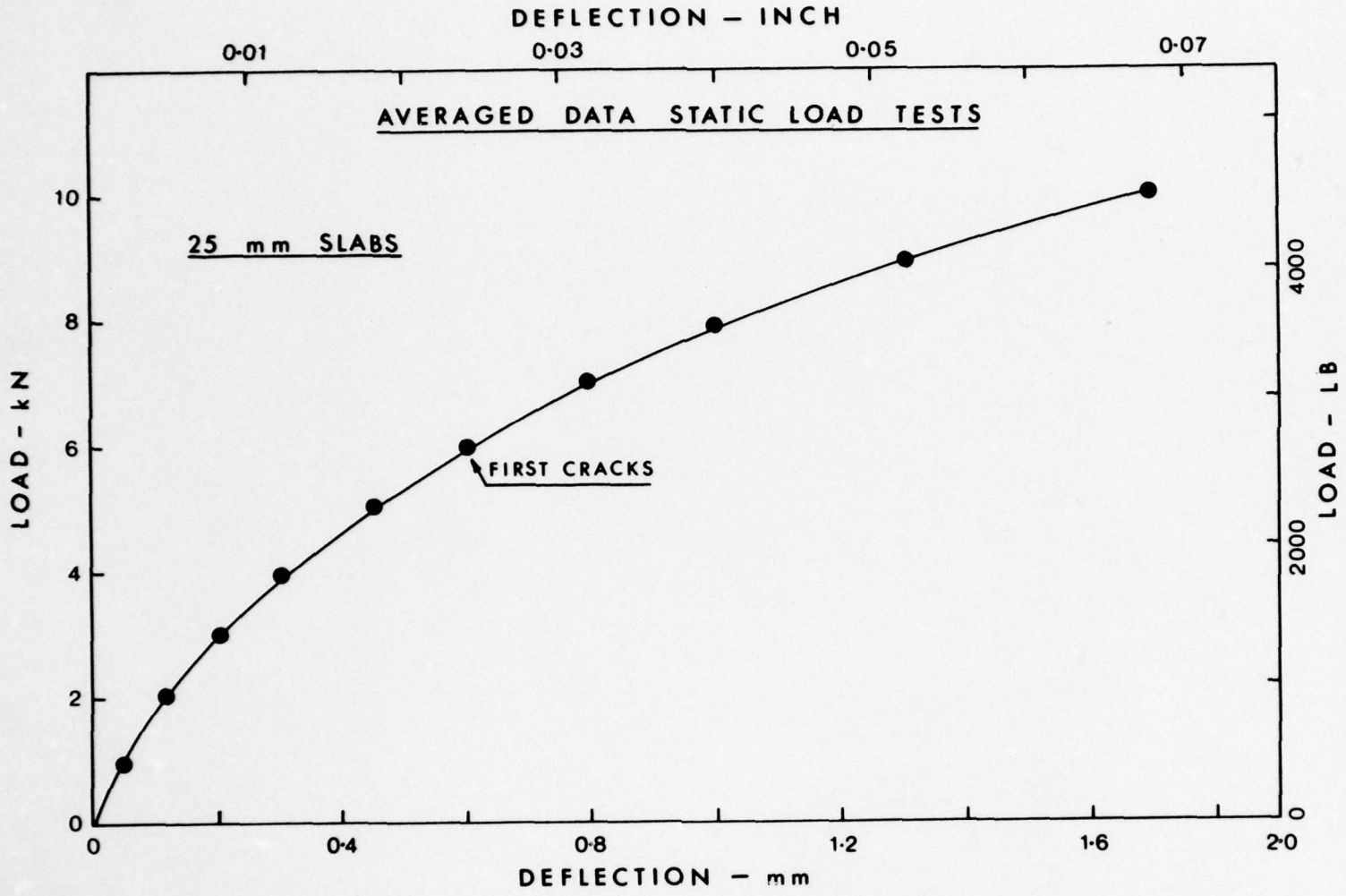

Fig III. 2

MID-SPAN DEFLECTION-VS-CENTRAL CONCENTRATED LOAD

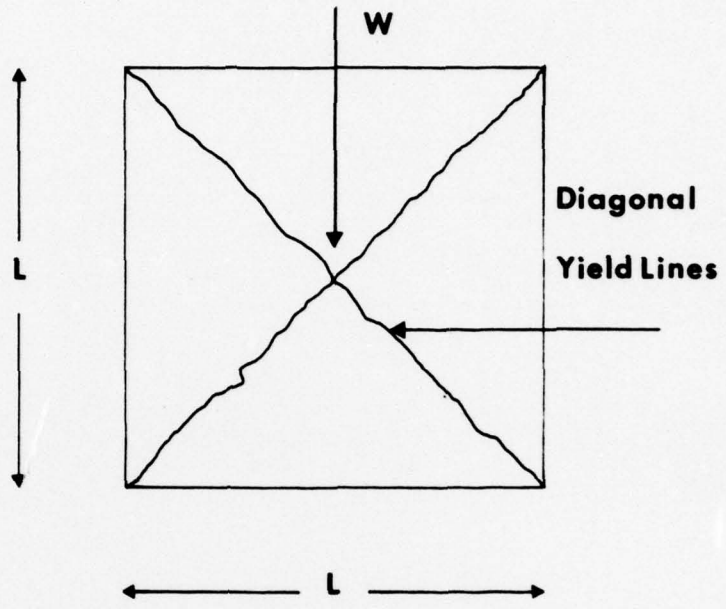

Fig IV.1 Slab at Collapse Load

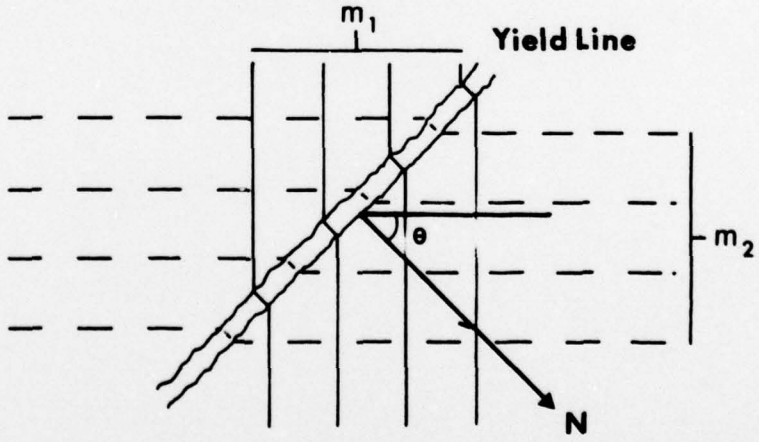

Fig IV.2

FIG IV GEOMETRY OF YIELD – LINES

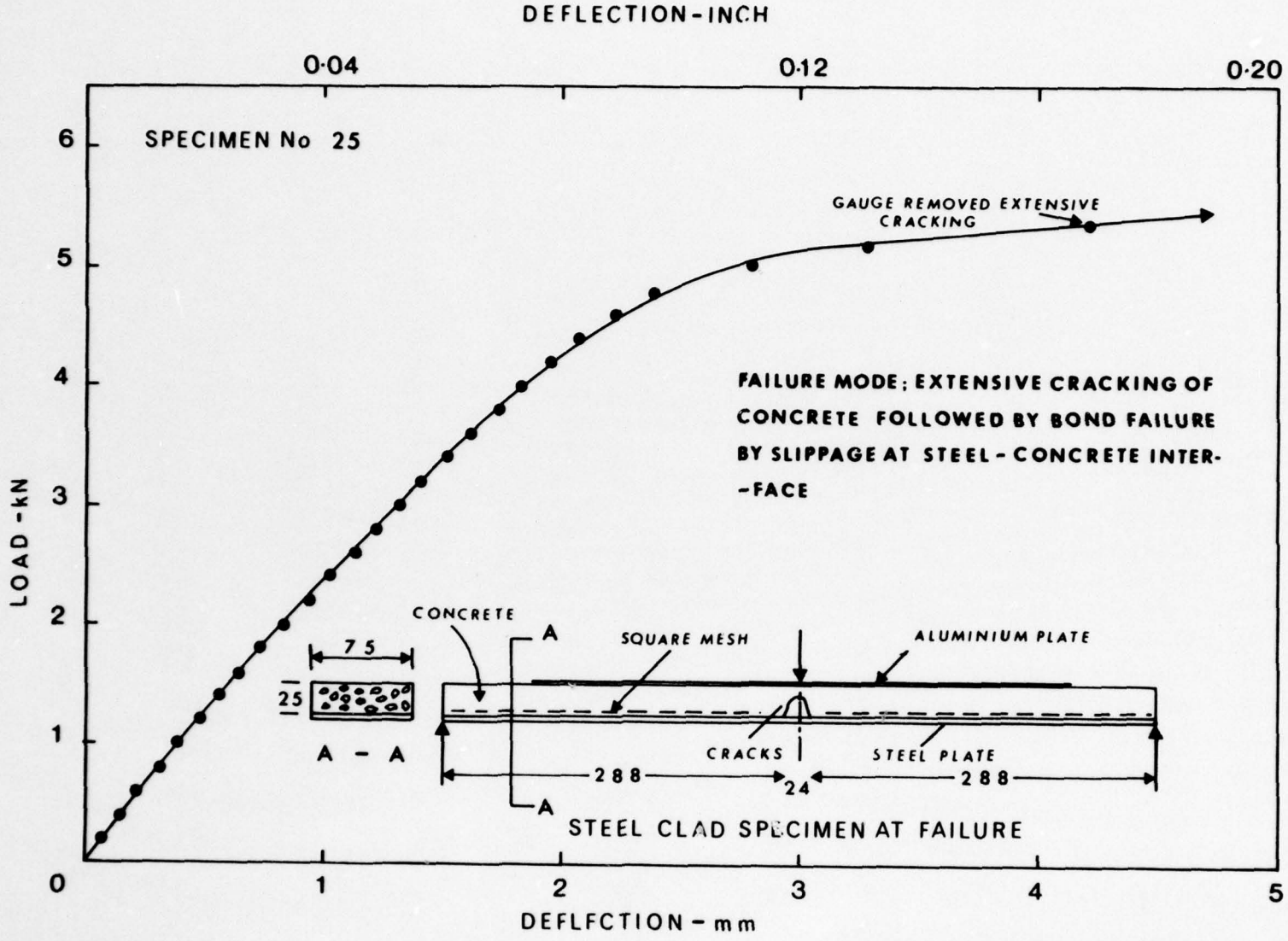

FIG V·2

CURVE OF LOAD-Vs-CENTRAL DEFLECTION

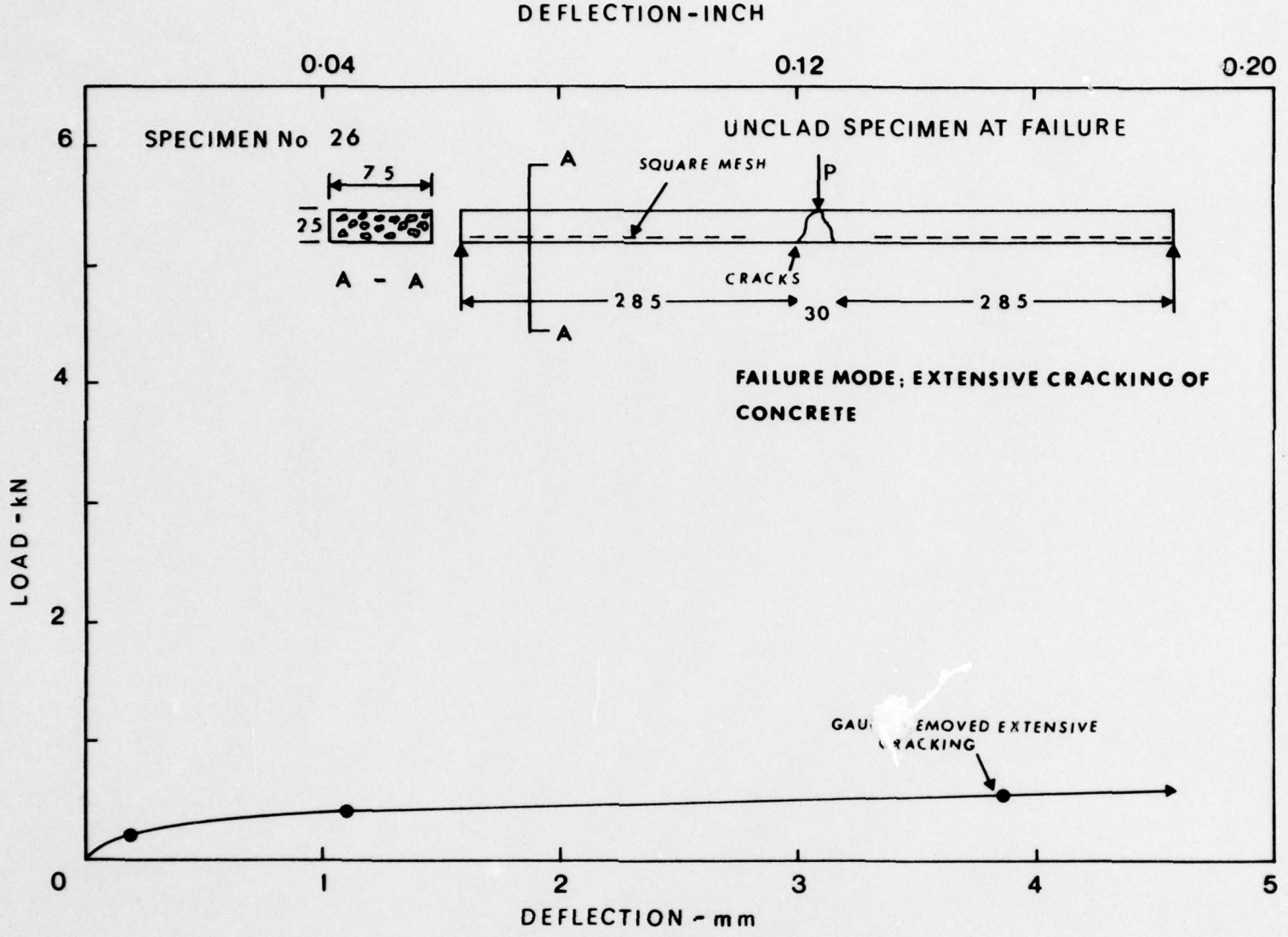

FIG 4.3

CURVE OF LOAD-Vs-CENTRAL DEFLECTION